Preserved Navigation abilities and Spatio-Temporal Memory in individuals with Autism Spectrum Disorder

Charles Laidi, Nathan Neu, Aurélie Watilliaux, Axelle Martinez-Teruel, Mihoby Razafinimanana, Jennifer Boisgontier, Sevan Hotier, Marc-antoine d'Albis, Richard Delorme, Anouck Amestoy, et al.

Title: Preserved Navigation abilities and Spatio-Temporal Memory in individuals with Autism Spectrum Disorder

Running Title: Preserved Navigation and Memory in adults with ASD

Authors

Charles Laidi [1,2,3,4], Nathan Neu [2,4], Aurélie Watilliaux [5], Axelle Martinez-Teruel [2], Mihoby Razafinimanana [5], Jennifer Boisgontier [4], Sevan Hotier [2,3], Marc-Antoine d'Albis [2,3,4], Richard Delorme [6], Anouck Amestoy [8], Štefan Holiga [7], Myriam Ly-Le Moal [8], Pierrick Coupé [9], Marion Leboyer [1,2,3], Josselin Houenou [1,2,3,4], Laure Rondi-Reig [5], Anne-Lise Paradis [5 *]

Affiliations

1: Univ Paris Est Créteil, INSERM U955, IMRB, Translational Neuro-Psychiatry, F-94010 Créteil, France
2: AP-HP, Hôpitaux Universitaires Henri Mondor, Département Médico-Universitaire de Psychiatrie et d'Addictologie (DMU IMPACT), Fédération Hospitalo-Universitaire de Médecine de Précision en Psychiatrie (FHU ADAPT) F-94010, France
3: Fondation FondaMental, Hôpital Albert Chenevier - Pôle de Psychiatrie, Créteil, France, F-94010 Créteil, France
4: UNIACT, Psychiatry Team, Neurospin Neuroimaging platform, CEA Saclay, (Gif-Sur-Yvette, France).
5: Sorbonne Université, CNRS, Inserm, IBPS, Neurosciences Paris Seine, CeZaMe Lab, 75005 Paris, France
6: Service de psychiatrie de l'enfant et de l'adolescent, Assistance Publique–Hôpitaux de Paris (AP-HP), Hôpital Robert Debré (Paris, France). Institut Pasteur, Human Genetics and Cognitive Functions Unit, Paris, France
7: Roche Innovation Center Basel | F. Hoffmann-La Roche Ltd | 4070 Basel | Switzerland
8: Institut Roche, Boulogne-Billancourt, France
9: Pictura Research Group, Laboratoire Bordelais de Recherche en Informatique, Unité Mixte de Recherche Centre National de la Recherche Scientifique (UMR 5800), University Bordeaux, Talence, France

*** *Corresponding author:*** 9, quai Saint-Bernard, case courier 16, F-75005 Paris.
anne-lise.paradis@upmc.fr

Conception and design: ALP, LRR, CL, StH, SeH, MLLM, JH, RD, ML

Data acquisition: CL, AMT, JB, StH, MAD, RD, ML, AA, JH, MLLM, SeH

Data analysis: CL, AW, ALP, NN, JH, PC, MR

Data interpretation: CL, LRR, ALP, AW, NN, MR

Original draft: CL, ALP, AW

Substantive revision: LRR, JH, MR

Acknowledgments

We thank SATT Lutech for their help in setting the software loan license agreement, Bérenger Thomas and Nadine Francis for their help in acquiring the data and Gregory Sedes for maintaining

NAT-H, our in-house developed software.

Fundings. This work was supported by the Investissements d'Avenir programs managed by the ANR under references ANR-11-IDEX-004-02 (Labex BioPsy) and ANR-10-COHO-10-01 and CNRS, and via collaboration with the Roche Institute for Research and Translational Medicine.

Competing interests. MLLM and StH are employees of F. Hoffmann-La Roche Ltd., which supported a part of the study. None of the authors received any fees from Roche for this study. The Virtual Starmaze has been registered under license number IDDN.FR.001.340006.000.S.P.2016.000.10000.

Lay Summary

In our study, adults with autism spectrum disorders (ASD) were able to learn and use different navigation strategies, similar to typically developing adults. Specific cerebellum regions needed for these abilities are thought to be affected in ASD. However, we found no difference in their volume or in their functioning at rest. Navigation and its associated brain circuits seem to be preserved in adults with ASD.

Abstract

Cerebellar abnormalities have been reported in autism spectrum disorder (ASD). Beyond its role in hallmark features of ASD, the cerebellum and its connectivity with forebrain structures also play a role in navigation. However, the current understanding of navigation abilities in ASD is equivocal, as is the impact of the disorder on the functional anatomy of the cerebellum. In the present study, we investigated the navigation behavior of a population of ASD and typically developing (TD) adults related to their brain anatomy as assessed by structural and functional MRI at rest. We used the Starmaze task, which permits assessing and distinguishing two complex navigation behaviors, one based on allocentric and the other on egocentric learning of a route with multiple decision points. Compared to TD controls, individuals with ASD showed similar exploration, learning, and strategy performance and preference. In addition, there was no difference in the structural or functional anatomy of the cerebellar circuits involved in navigation between the two groups. The findings of our work suggest that navigation abilities, spatio-temporal memory, and their underlying circuits are preserved in individuals with ASD.

Keywords: Autism Spectrum Disorder, Spatial Navigation, Cerebellum, Memory, Adults

1. Introduction

Despite great heterogeneity in autism spectrum disorders (ASD), MRI studies have reported consistent structural and functional atypicalities in cortical regions, such as the superior temporal sulcus and inferior frontal gyrus (Bedford et al., 2020; Holiga et al., 2019). Disconnectivity between cortical regions (Khan et al., 2015), more specifically the temporoparietal junction (Igelström et al., 2017; Stoodley et al., 2017), and posterior cerebellar cognitive regions (typically Crus I and II), has also been reported in children and adolescents. In addition, a large body of literature, including histopathology, genetics, neuroimaging (see Fatemi, 2013; Wang et al., 2014; and D'Mello et al., 2015 for a full review), and pre-clinical studies (Kelly et al., 2020; Stoodley et al., 2017), suggests that cerebellar alterations play a role in the pathophysiology of ASD. Collectively, this literature supports the concept that the cerebellum and the behaviors it underlies may be altered in ASD.

The cerebellum is involved in a broad range of social (Van Overwalle et al., 2014; Van Overwalle et al., 2015), and repetitive / restrictive behaviors (RRB) (Stoodley et al., 2017; Dean et al., 2022), which are the hallmark features of ASD. Beyond social cognition and RRB, the cerebellum is also known to be involved in a broad range of cognitive functions (Schmahmann, 1998; Schmahmann & Caplan, 2006; Stoodley et al., 2012), including spatial navigation.

Our group has contributed toward revealing the cerebellum to be a key structure in the spatial navigation system (review in Rondi-Reig & Burguière, 2005; Rondi-Reig et al., 2014; Burguière et al., 2005; Iglói et al., 2015; see also Petrosini et al., 1998). In rodents, intact cerebellar computation is required for stabilizing hippocampal spatial representation maps and for goal-directed navigation (Rochefort et al., 2011; Lefort et al., 2019). We further reported that a hippocampo-cerebellar-prefrontal centered network sustained the learning and execution of goal-directed navigation based on route memory (Babayan et al., 2017). Functional MRI studies in humans also revealed similar results with a specific involvement of the right cerebellar lobule VIIA Crus I (RCrusI) and its functional connectivity with the prefrontal cortex and the hippocampus when the participants relied on route memory to reach their goal (Iglói et al., 2015). In addition, we also observed Left Crus I (LCrusI) along with medial parietal activation when participants relied on allocentric representation. With the involvement of the cerebellum in both ASD and navigation, it can be expected that the navigation abilities may be impaired in ASD.

Few studies have investigated the navigation abilities of individuals with ASD, and the findings appear contradictory. While some studies documented that individuals with ASD had impaired ability to learn location based on allocentric representations or to explore their

environment compared to individuals with typical development (TD), others reported similar learning when the task involved simple place learning or egocentric route learning. Some reports even suggested a better recall or learning of routes in ASD when using maps (see Smith, 2015 for a full review). Thus, the knowledge of navigation in ASD is ambiguous, and an extensive evaluation of navigation behavior and its underlying circuits is necessary to determine the navigational ability of individuals with ASD.

The task used to assess navigation behavior is critical. Originally designed to study spatial learning and memory (Olton & Samuelson, 1976), the radial arm maze that has been used to evaluate mouse models of ASD (Rendall et al., 2016), is ideal to distinguish place-based from response-based navigation strategies (see review in Palombi et al., 2022). However, consisting of eight arms radiating from a central circular platform, the radial arm maze offers only one decision point in the center of the maze and does not assess the ability to acquire the memory of a complex route. The Starmaze, with a structure based on the presence of central alleys, allows the testing of paths with multiple decision points, closer to the real-life navigation. It, thus, makes it possible to test and distinguish egocentric route learning (also called sequence-based) and allocentric learning (also known as map- or place-based) in a single environment (Rondi-Reig et al., 2006). By introducing a sequential organization into navigation decisions, this configuration also allows testing the temporal component of navigation in addition to the spatial one (Fouquet et al., 2010). Validated in rodents (Fouquet et al., 2010), TD humans (Iglói et al., 2009, Bullens et al. 2010) and individuals with Alzheimer's disease or fronto-temporal dementia (Bellassen et al. 2012), and used to evaluate the effectiveness of a navigation training (van der Kuil et al., 2020), the Starmaze also highlighted some neurobiological underpinning of place- and sequence-based strategies (Iglói et al., 2010, 2015). Hence, the Starmaze is a better paradigm for examining place- and sequence-based navigations in the same environment.

Taking advantage of the Starmaze task, we investigated both the egocentric and allocentric learning of ASD individuals in relation to their brain anatomy. Given the involvement of the cerebellum in both ASD and navigation, we expected deficits in the acquisition of the sequence-based strategy associated with impaired RCrusI-prefrontal circuits in individuals with ASD. We additionally expected impaired allocentric learning and internal representations associated with altered LCrusI-parietal connectivity in people with ASD compared to TD individuals.

2. Material and methods

Participants

We recruited adults with ASD from the Mondor University Hospital (Créteil, France) and TD individuals through advertisements in the local press. For individuals with ASD, diagnoses were confirmed by trained clinicians, and using the Autism Diagnostic Interview-Revised and the Autism Diagnostic Observation Schedule. All recruited participants were above 18 years, had no history of intellectual disability, neurological disorder, or alcohol abuse or dependence, except for tobacco. Individuals with a personal history of axis I disorder or a first-degree relative with schizophrenia, schizoaffective, or bipolar disorder were not included as TD controls.

Participants with ASD underwent an IQ assessment with the WAIS-IV scale. TD participants underwent the Kaufman Brief Intelligence Test-2, and the National Adult Reading Test (Nelson, 1982) in Créteil. Individuals with ASD and TD adults underwent a standardized cognitive assessment (Test of Attentional Performance, Psytest), exploring working memory, verbal flexibility, divided attention, response inhibition, and shifting of attentional focus to ensure that both groups had similar general cognitive performance (Table 1 and Supplementary Material S7). The details are as described elsewhere (Laidi et al., 2017).

In all, 30 individuals with ASD and 32 TD adults underwent a full navigation assessment with the virtual Starmaze and MRI on the same day, including structural and resting-state sequences (Supplementary Material S1). This exploratory study is part of the observational clinical study C07-33 sponsored by Inserm. It was granted approval by the local Ethics Committee or “Comité de Protection des Personnes” on November 18, 2008, authorized by the French authorities (AFSSAPS B80738-70, August 11, 2008), and registered in a public registry (NCT02628808). All study participants gave their informed written consent to participation, in line with the French ethical guidelines.

Virtual Starmaze task

The virtual Starmaze environment (registered under license number IIDN. IDDN.FR.001.340006.000.S.P.2016.000.10000) was built with Blender software (version 2.76b for Windows). The task was run on a windows laptop (processor Intel i7, 8 Go RAM, NVIDIA graphic card), and displayed on a separate 17” LCD monitor, using a joystick (Logitech Attack 3) to move within the virtual environment.

The environment is a star-shaped maze, consisting of five central alleys forming a pentagon,

and five peripheral alleys starting from the vertices of the pentagon. Alleys were materialized with a different floor texture and side walls preventing exit from the maze. The height of the external walls allowed the participants to see the distal landmarks (extra-maze cues) placed around the maze, but the central walls were higher to prevent the participants from seeing the alleys beyond the central pentagon (see views from the start points on Figure 1), and having an overview of the general shape of the maze.

There were eight landmarks consisting of four doubled items (two each of mountains, forests, antennas, and villages). Doubles were slightly different in appearance and in their spatial configuration with respect to the other landmarks. They were placed on opposite sides of the environment so that the participants could never see them together. There were no intra-maze cues except for the walls forming the internal pentagon at the center of the maze, which had a contrasting texture compared to the outer walls, to facilitate the interpretation of the global maze configuration.

Participants were instructed that a virtual gift was hidden in the environment and would show up only when they reached the right place. They were also informed that the reward location did not change. At the beginning of each trial, participants were virtually located in a peripheral alley and heading toward the maze center.

Pre-training. After a short demonstration of how to manipulate the joystick, the participants were invited to use it to move around the virtual environment. The environment used for this pre-training was a Y maze with no landscape. Once the participants felt at ease with the use of the joystick, we tested their ability to control their movements in the virtual environment by asking them to reach a visible flag (Motor control condition, Figure 1). The environment was such that they had to undertake several turns on their way to the goal.

Training. The participants were instructed that compared to the pre-training, the environment would change, and that they would have to explore this new environment to find the place where a hidden gift would show up. After the first trial they were asked to go to the reward location as directly as possible (without detours). Trials were limited to 2 min. For the first three trials, if they did not find the reward location in the allotted time, they were teleported at the entrance of the rewarded alley and asked to follow an arrow on the ground until the gift appeared. In total, participants underwent five training trials in the Starmaze environment. Next, they were offered a short pause (about 2 min) during which we collected personal information, such as laterality, age and education level. The interview also served as an interfering task to ensure that

the participants did not retain the task in working memory before the test session.

Test session. After the pause, the participants underwent a test session. Navigation behavior involves both egocentric (i.e. encoded in the reference frame of the subject) and allocentric (i.e. in the reference frame of the environment) representations. Individuals relying on an egocentric representation are expected to reproduce the learned route (sequence-based strategy) while those relying on an allocentric representation will orient themselves with respect to landmarks (place-based strategy). To characterize the navigation abilities and preference of the participants in the Starmaze, the test session included trials designed to assess egocentric ("Ego Trials") and allocentric ("Allo trials") learning as well as the type of strategy spontaneously favored by the participants ("Probe trials"). In summary, this session consisted of: (i) a training trial aimed at testing how well the spatio-temporal memory has been acquired;

(ii) two probe tests (Figure 1, Probes 1 and 2) in which participants started from a different place without being told, in order to determine whether, in this case, the participants would spontaneously locate the reward with respect to the external landmarks (place-based strategy) or reproduce the path learned during the training without taking into account the external landmarks (sequence-based strategy). Both the strategies were rewarded;

(iii) a training trial followed by an 'Ego' trial without landscape (Figure 1, Ego) to test the ability of the participants to reproduce the memorized sequence in the absence of distal visual landmarks. Before this Ego trial, participants were instructed that the landmarks would not be available anymore but that their goal and departure points would be the same as usual so that they could rely on the path they had learned (forced use of the sequence-based strategy);

(iv) an 'Allo' trial in which the participants were explicitly told they would start from a different departure (Figure 1, Allo a), to test their ability to use the visual landmarks rather than a memorized path to find the goal place. On this Allo trial, only the actual place of the goal was rewarded, such that the participants had to use the place-based strategy to succeed (forced use of the place-based strategy). Last participants had an additional Allo trial (Figure 1, Allo b), which was not further analyzed in the present study.

Post-experiment interview. After the computer session, participants were asked to 1) recognize the shape of the visited maze among different propositions presented on a paper sheet; 2) draw their path to the gift on a map of the correct maze, from a starting point positioned in front of them; 3) cite all the visual cues they had perceived outside the maze and could freely recall; 4) place the visual cues on the map of the maze relative to the gift position.

Navigation scores

The virtual Starmaze records the position and orientation of the participants in the environment every 100 ms. We thus have access to their point by point trajectory and are able to compute various navigation scores at each trial using an in-house developed software (registered under license number IIDN. FR.001.160024.000.S.P.2017.000.10000).

To assess the successful learning of the task, we checked whether the participants were able to reach the goal in a minimal number of alleys by the end of the training phase. Those who were not able to get to the goal directly (4 alleys, Figure 1 right panel) or with minimal detour (5 alleys) at least twice between training trials 4 and 6 were considered as non-learners and excluded from further analysis.

We computed (i) the localization index, which is the proportion of correct turns over all visited intersections, and thus evaluates the ability of the participants to turn toward the goal direction at each intersection of the maze and (ii) the mean traveling speed, which depends on a trade-off between self-motion optimization and visual exploration, and allows to monitor learning independently of the path traveled. These scores were used to assess and compare the acquisition of the Starmaze task in both ASD and TD groups.

To control for possible visuo-motor deficits that may interfere with the navigation assessment, we compared the participants' mean speed in the motor control condition. Because the cerebellum has been documented to be involved in the ability to optimize trajectories (Burguière et al., 2005), we computed the optimization of the distance. This score (minimal distance to reach the goal from the departure divided by the actual distance traveled; ranging from 0 to 1) assesses the ability of the participants to produce an accurate movement.

For each participant, we identified the type of strategy favored at the Probe trials. The spontaneous strategies were classified as sequence-based if the participants reproduced the learned path ("sequence" for the direct path, "long path" for the 5-alley path getting around the center of the maze in Figures 2.E and 2.H), place-based if the individuals directly headed toward the goal place as defined by the environmental cues, or "mixed" if the individuals began with reproducing their usual path and corrected their trajectory on the way to directly reach the goal without any entrance in a wrong peripheral alley. Other types of trajectories were labeled "other".

We then assessed the participants when they were forced to use a specific strategy, thus evaluating their ability to navigate directly to the goal in the Allo a trial (departure point explicitly

modified to force the use of place-based strategy) and reproduce the learned path in the Ego trial (suppression of the distal visual cues to force the use of the sequence-based strategy).

Based on the post-experiment interview, we assessed the internal representation of the participants. This included their ability to recognize the shape of the visited maze among different propositions, the number of landmarks they could recall freely, the number they could correctly place on a maze map (to evaluate this we checked whether the locations pointed by the participants for each item fell in the correct areas of a pre-established reference scheme), and the number of doubled landmarks they noticed. This also included their ability to reproduce their learned path on the maze map (drawing passing reproducing the correct succession of alleys from start point to goal alley = 1; everything else = 0).

To test a possible association of the navigation behavior with anatomy and functional connectivity at rest, we further selected three scores reflecting three main aspects of navigation: Exploration speed, Allocentric success standing for the ability to use place-based navigation when forced to, and Egocentric score standing for the ability and tendency to use sequence-based navigation (See Supplementary Material S2.a).

MRI data

Participants underwent both structural and resting-state functional MRI. We performed a volumetric analysis of Cerebellar Crus I (bilateral, left, right) in 17 ASD and 22 TD participants, and studied its functional connectivity in 16 ASD and 22 TD participants (see Supplementary Material S1 depicting the flowchart of the number of individuals per group). Based on the results of Iglói et al. (2015), we focused the connectivity analysis on three pairs of structures: LCrusI - parietal cortex, which we found to be involved in place-based strategy; RCrusI - left hippocampus and RCrusI - medial PFC, which were involved in sequence-based strategy (Iglói et al., 2015). Their functional connectivity was calculated as a Spearman correlation between their resting-state functional MRI time series. We then tested the association of volume or functional connectivity with the navigation scores reflecting place-based, sequence-based, or exploration behavior (see Supplementary Material S2.b-e for detailed methods of MRI data analysis).

Statistical analyses

Bayesian approach. The traditional frequentist statistical approach is particularly appropriate for reporting results that lead to rejecting the null hypothesis. However, no conclusion can be drawn in case no significant difference is observed. Given the mixed results reported in

the literature about differences of visuo-spatial skills between TD and ASD, it was essential to be able to report positive and negative results. We, therefore, applied a Bayesian approach, which allows to argue in favor of the null hypothesis as well as the alternative hypothesis (Keysers et al., 2020). The method provides a Bayesian Factor (BF) as a result of the analysis:

- BF_{01} is reported for analyses with only one factor (e.g. t-tests) and indicates how many times the data is more likely to satisfy the null hypothesis over the alternative hypothesis;

- BF_{excl} is reported for analyses including more than one factor (e.g. ANOVAs) and indicates how many times the models that do not include a specific factor are more likely to explain the data than models including that factor.

BF_{01} or BF_{excl} above 1 are interpreted in favor of the null hypothesis with anecdotal ($2<BF<3$), moderate ($3<BF<10$), strong ($10<BF<30$), very strong ($30<BF<100$) or extreme ($BF>100$) evidence. BF below 1 are interpreted in favor of the alternate hypothesis with anecdotal ($1/2>BF>1/3$), moderate ($1/3>BF>1/10$), strong ($1/10>BF>1/30$), very strong ($1/30>BF>1/100$) or extreme ($BF<1/100$) evidence. With BFs between 1/2 and 2, we consider that no conclusion can be drawn (adapted from Jeffreys, 1961). The results of the frequentist statistics are provided as Supplementary Material S5. All analyses were undertaken using JASP software (0.16.0.0) (Goss-Sampson, 2020).

Behavioral testing. Because the score values did not follow normal distributions, we used non-parametric Mann-Whitney tests to compare the performance of the two groups during the motor control condition (mean speed and distance optimization score, Figure 2); and on the recall and the placement of cues based on the post-experiment interview (Figure 3). Ten thousand samples were performed for each of these tests, to obtain a more stable Bayesian factor (Goss-Sampson, 2020).

To compare the mean speed and localization score of the two groups across the trials of the training phase, we used two-factor ANOVAs (Group: ASD vs. TD x Trial: 1,2,3,4,5), with comparisons of effects across the matched models to provide a better estimate of the contribution of each factor (Keysers et al., 2020).

To determine whether groups differed in their strategy on probe trials (place-based vs. sequence-based), and their success on Allo trial, Ego trial, Drawn path (Figure 2) or maze recognition (Figure 3), we used Chi-square tests with an independent multinomial sampling method (Goss-Sampson, 2020).

MRI Data analysis. ANCOVAs were used to determine if the volume of the cerebellum Crus I could be linked to the diagnostic group and navigation score as fixed factors, while controlling for age, sex, and intracranial volume, included as covariates. We also performed ANCOVAs to test the association between the functional connectivity of our structures of interest (dependent variable) with the navigation score, diagnostic group, and sex, included as fixed factors. Age and mean frame displacement were included as covariates. Additionally, the methods used for frequentist statistical analyses have been provided as Supplementary Material S2.f.

3. Results

Navigation behavior

Participants in both ASD and TD groups succeeded in learning the Starmaze task, with the majority (24 ASD, 26 TD) being able to reach the goal at least twice between trials 4 and 6 with the minimal number of alleys (4, see Figure 1 right panel), and four subjects in each group learned with a small detour (one more alley) (Figure 2A). Three individuals, two ASD and one TD, failed to fulfill the learning criterion and were excluded from the subsequent analyses. Thus, 28 individuals with ASD and 31 neurotypical subjects were included in the behavioral analyses. The demographic characteristics of the participants are depicted in Table 1. There was no significant difference between the two groups in terms of age and sex ratio. All results obtained using Bayesian statistics are described in detail below, and the frequentist statistics undertaken are available as Supplementary Material S5.

The motor control condition revealed anecdotal to moderate evidence in favor of an absence of difference between groups in distance optimization (BF_{01} = 2.22, ASD: median = 0.910 [0.905, 0.912] vs. TD: median = 0.911 [0.902, 0.914]) and mean speed (BF_{01} = 3.01, ASD: median = 0.613 [0.545, 0.653] vs. TD: median = 0.591 [0.513, 0.640]) (Figure 2B).

Along the training phase, we found extreme evidence in favor of a trial effect for both the localization score (LocS: BF_{excl} = 1.07e-39) and mean speed (MS: BF_{excl} = 3.14e-43). By contrast, respectively, moderate and strong evidence supports an absence of Group effect (LocS: BF_{excl} = 3.07; MS: BF_{excl} = 3.26) and interaction (LocS: BF_{excl} = 19.14; MS: BF_{excl} = 5.50), suggesting similar learning in the two groups (Figures 2C and D). Post-hoc t-tests revealed that a plateau was reached as soon as the third trial for the localization score with anecdotal to moderate evidence of no trial effects from T3 to T5 ($BF_{01,U}$: T3 vs. T4 = 2.61; $BF_{01,U}$: T3 vs. T5 = 1.69; $BF_{01,U}$: T4 vs. T5 = 4.72).

In the first probe trial, which displayed a starting view similar to that of the previous training trials, most participants (23 ASD, 25 TD) reproduced the path learned at the end of the training. Only one participant in the ASD group and four from TD group headed toward the goal place directly or after a small detour along their preferred path. On comparing the proportions of individuals using a sequence-based strategy (reproducing their direct sequence or long path, 23 ASD and 25 TD) with those relying on visual cues (place-based or mixed, one ASD and four TD), we found anecdotal evidence in favor of an absence of difference between ASD and TD groups (BF_{01} Independent multinomial = 2.76, Figure 2E).

All participants whose strategy was labeled “other” visited only one wrong peripheral alley before reaching the goal alley, suggesting they did not completely re-explore the maze and rather relied on visual cues to find the goal. If we group these individuals with those using a place-based or mixed strategy (total proportion in ASD: 18% vs. TD: 19%), the evidence in favor of no group effect increases to moderate (BF_{01} Independent multinomial = 4).

In the second probe trial, we also found moderate evidence for no group effect. Whether or not strategies labeled “other” were included, the proportion of participants relying on visual cues was similar in the ASD and TD groups (place-based and mixed strategies: 28% in ASD vs. 25% in TD, BF_{01} Independent multinomial = 3.31; place-based, mixed and “other” strategies: 36% in ASD vs. 32% in TD, BF_{01} Independent multinomial = 3.22).

In the Allo trial, the two groups showed the same percentage of successful participants (10 ASD and 13 TD, Figure 2F), with anecdotal evidence supporting the absence of any difference (BF_{01} Independent multinomial = 2.90).

As regards the Ego trial, the percentage of successful participants was very high and not significantly different between the groups (with 26 ASD and 27 TD, Figure 2G), with moderate evidence in favor of the null hypothesis (BF_{01} Independent multinomial = 5.25).

The analysis of the drawn path showed consistent results, with a very-high percentage of success (ASD: 93%, TD: 84%, Figure 2G), and no significant difference between the groups (BF_{01} Independent multinomial = 2.91).

Overall, participants in ASD and TD groups showed very similar performance and used the same type of strategy in similar proportions. In particular, there was no significant difference in the three scores that were also used to test their possible link with the volume and the resting-state connectivity of Crus I: exploration speed (Figure 2D, trial T1), allocentric success (Figure

2F) and egocentric score (Figure 2E, Probe 2 DV, direct and long path in green).

Post-experiment interview

Participants mostly chose the correct maze among the six (Figure 3A, maze E: 82% in ASD and 84% in TD), with moderate evidence of no difference between ASD and TD in terms of success (BF01 Independent multinomial = 4.11). Additionally, ASD and TD remembered the same number of landmarks (total number in Figure 3B, ASD: median = 4 [4, 5]; TD: median = 4 [4, 5]; anecdotal evidence with BF_{01} = 2.85) and did not notice a different number of doubles (median = 0.5 [0, 1]; TD: median = 1 [0, 2]; anecdotal evidence with BF_{01} = 2.42). Further, there is moderate evidence in favor of no difference between the groups with regards to the number of landmarks correctly placed around the map of maze (Figure 3C, ASD: median = 3 [2, 4]; TD: median = 2 [1, 4]; BF_{01} = 3.18).

Crus I volume and functional connectivity

In this anatomical analysis (17 ASD, 22 TD, see Supplementary Material S2g for demographic characteristics), there was no significant effect of individuals' ability to perform a navigation strategy (Egocentric score or allocentric success), or of the diagnostic category, or of interaction between the two on the volume of Crus I (Supplementary Material S3.a-b). Similar to our previous results at the level of the global volume (Traut et al., 2018), no significant difference of Crus I volume in participants with ASD compared to controls (Supplementary Material S3.c) was noted.

Likewise, in the resting-state analysis (16 ASD and 24 TD, see Supplementary S2.h for demographic characteristics), we found no significant effect of navigation strategy, diagnosis or their interaction on the cerebellum-hippocampus-prefrontal-parietal connectivity (Figure 4 and Supplementary Material S4.a-b)

4. Discussion

We studied spatial navigation with a paradigm validated in rodents and human adults (Burguière et al., 2005; Iglói et al., 2009a), children (Bullens et al., 2010), as well as older patients with mild cognitive impairments, Alzheimer's disease, and fronto-temporal dementia (Bellassen et al., 2012). Except for three individuals (two with ASD and one TD), all participants from the two groups completed our behavioral task, suggesting that they understood it well and could learn similarly.

When comparing the two groups, there was no difference in terms of the navigation strategies. In addition, we found that there were no difference in the circuits involved in spatial navigation in ASD and TD, suggesting that there are neither striking differences in navigation behavior nor anatomical atypicalities in the underlying circuits. As the sample size of our study was limited, our negative findings might be related to a lack of power. However, the use of Bayesian statistics provides an argument for no difference. Furthermore, with the same task and smaller sample sizes, our group had earlier reported robust navigation and memory alterations in Alzheimer's disease (Bellassen et al., 2012). This suggests that, if present, spatial navigation abnormalities are subtle in ASD.

In line with our findings, a review by Smith (2015) reported no significant difference in ASD and TD with a large number of spatial navigation tasks (including elements of path integration, route learning, and simple place learning). The author also reported improved perceptual distance matching and cued recall of routes on a map for ASD compared to TD, but it may be noted that these abilities were not tested in our study. In contrast, the review had also reported impairments in ASD in the exploration of the environment, or the ability to learn locations based on allocentric representation. In a study by Lind et al. (2013), the authors found impaired survey-based navigation skills in the memory island virtual navigation task, suggesting difficulties generating cognitive maps of the environment. Similar impairments have also been reported with a computerized virtual Morris water maze in adults with ASD (Ring et al., 2018).

In the present study, the participants' ability to perform place-based strategy as well as their memories of the maze after the task, even when tested on subtleties such as doubled landmarks, suggest that ASD adults do not have allocentric learning deficits or impaired internal representations. Compared with our task, the memory island task begins training with visible goals so that the four trials with invisible goals, on which participants are tested, not only require memory

of the environment but also cognitive flexibility to learn the new task in a few trials. Moreover, the environment of the memory island is voluntarily rich, including not only visual but also auditory stimuli. Considering the atypical sensitivity of some individuals with ASD to sensory inputs, the simultaneous stimulation of multiple modalities might reveal overwhelming and increase the difficulty of the task.

Classically, open mazes, such as the Morris water maze or the memory island, are contrasted with corridor mazes in terms of the neural circuits involved. While the acquisition of the former is known to involve the hippocampus, that of the latter is speculated to be centered on the caudate nucleus. According to Lind et al. (2013) this may be the reason why ASD individuals are impaired in the survey-based strategy but not in the route-based strategy in corridor mazes as noted by Caron et al. (2004). However, although the Starmaze is a corridor maze, as the radial-arm maze, it is noteworthy that both the sequence-based and place-based strategies used to acquire this task were found to involve the hippocampus (Iglói et al., 2010; 2015). Thus, although the presence of corridors or walls structuring the maze could be an important point to explain the different results of spatial memory studies in ASD, our results in the Starmaze suggest that it is not related to the hippocampal involvement.

The constraints of the corridors may impact the difficulty of the memory task per se by limiting the number of potential goal locations. Although we cannot exclude that a lower difficulty of our task may mitigate the effects of possible impairments, the lack of a difference in the ability to correctly place landmarks on a map of the maze suggests that the internal representation of the virtual environment is not less accurate in individuals with ASD.

The presence of guiding corridors may also mask the impact of possible deficits in movement accuracy on the ability to reach the goal location. However, when testing their ability to optimize the traveled distance during the motor control trial, we noted that there was no difference in movement accuracy between individuals with ASD and TD adults when they had to reach a visible goal. We also found that there was no significant difference with an invisible goal, when the participants performed their learned path in the navigation task (see Supplementary Material S6.a). To further ensure that the mere presence of visual landmarks could not serve as visual targets and help movement accuracy in ASD individuals, we confirmed that they did not travel a larger distance than TD individuals when they reproduced the learned path in the absence of landmarks (Ego trial, see Supplementary Material S6.b).

The lack of observable impact of ASD on landmark representation or movement accuracy suggests that the difficulties reported in open mazes are not related to specific deficits in motor optimization or hippocampal representation. Instead, we suggest that the corridors may alleviate the burden of sensory-motor integration by helping the navigators focus the task on the acquisition of spatio-temporal memory rather than the precise online monitoring of self-movement along with visual information.

Functional MRI studies have reported disconnectivity between the cerebellar cognitive regions (typically Crus I and Crus II) and the associative cortex (Khan et al., 2015) in children and adolescents with ASD, more specifically in the temporo-parietal junction (Igelström et al., 2017; Stoodley et al., 2017). Functional resting-state atypicalities have been evidenced in autism (Holiga et al., 2019), with hypo-connectivity in sensory-motor regions as well as hyper-connectivity in the prefrontal and parietal cortices. However, based on our information, this study is the first to focus specifically on the networks involved in spatial navigation in ASD individuals compared to TD adults.

Although task-free MRI can predict individual differences in brain activity during task performance (Tavor et al., 2016), we found no difference between ASD and TD or in relation to the task in terms of the structural or functional anatomy of the cerebro-cerebellar circuits involved in spatial navigation. The absence of difference between the groups is in line with a previous meta-analysis that included a large dataset of individuals with ASD (Di Martino et al., 2017), wherein we found no significant difference in cerebellar morphology in ASD compared to controls on a grosser scale (Traut et al., 2018). The finding that the navigation scores do not contribute to neuroimaging features in the participants who learned the task is also similar to a recent cohort study that showed only a small correlation between task performance and fMRI activations, even though these were task-related and the sample size was larger (Chaarani et al. 2021).

Unlike MRI assessment performed during a spatial navigation task (Iglói et al., 2015), structural MRI and resting-state functional connectivity do not allow studying the dynamics of cerebellar activation or network reorganization with learning. Our results thus suggest that “off-line” MRI assessment is insufficient to investigate the involvement of the cerebellum in spatial navigation, at least when learning is globally efficient. Hence, it would be relevant for future studies to use MRI during a task or to test structural and functional anatomy against significant behavioral deficits that perhaps target multisensory integration.

To the best of our knowledge, our study is the first to investigate spatial navigation in ASD, which incorporated both behavioral and neuroimaging data. Our results did not reveal differences between ASD and TD participants in their navigation behavior, internal representation, or underlying neural circuits. ASD participants were even able to switch from one strategy to another when both had been learned together. This suggests that the navigation difficulties sometimes reported for ASD individuals are related to upstream multisensory information intake, which is alleviated in structured environments, rather than their spatiotemporal memory or the implementation of specific strategies. Regarding cerebellar connectivity in ASD, a more exhaustive assessment would require exploring a larger cohort and assessing functional connectivity during a task (as in Iglói et al., 2015). 7T MRI might be more relevant as well to increase the spatial resolution, especially in the cerebellum, where the cortical foliation could be studied more deeply (Sereno et al., 2020). However, the absence of neuroimaging differences between ASD and TD strengthens our results on behavior and further implies that there are no striking abnormalities in the neural basis of spatial navigation in individuals with ASD.

List of abbreviations

Allo: Allocentric

ASD: Autism Spectrum Disorders

Ego: Egocentric

MRI: Magnetic Resonance Imaging

TD: Typical Development

References

Babayan, B. M., Watilliaux, A., Viejo, G., Paradis, A.-L. L., Girard, B., & Rondi-Reig, L. (2017). A hippocampo-cerebellar centred network for the learning and execution of sequence-based navigation. *Scientific Reports*, 7(1), 17812. https://doi.org/10.1038/s41598-017-18004-7

Bedford, S. A., Park, M., Devenyi, G. A., Tullo, S., Germann, J., Patel, R., Anagnostou, E., Baron-Cohen, S., Bullmore, E. T., Chura, L. R., Craig, M. C., Ecker, C., Floris, D. L., Holt, R. J., Lenroot, R., Lerch, J. P., Lombardo, M. V., Murphy, D., Raznahan, A., Ruigrok, A., … Chakravarty, M. M. (2020). Large-scale analyses of the relationship between sex, age and intelligence quotient heterogeneity and cortical morphometry in autism spectrum disorder. *Molecular psychiatry*, *25*(3), 614–628. https://doi.org/10.1038/s41380-019-0420-6

Bellassen, V., Iglói, K., de Souza, L. C., Dubois, B., & Rondi-Reig, L. (2012). Temporal order memory assessed during spatiotemporal navigation as a behavioral cognitive marker for differential Alzheimer's disease diagnosis. *The Journal of Neuroscience: The Official Journal of the Society for Neuroscience*, *32*(6), 1942-1952. https://doi.org/10.1523/JNEUROSCI.4556-11.2012

Bullens, J., Iglói, K., Berthoz, A., Postma, A., & Rondi-Reig, L. (2010). Developmental time course of the acquisition of sequential egocentric and allocentric navigation strategies. *Journal of Experimental Child Psychology*, *107*(3), 337-350. https://doi.org/10.1016/j.jecp.2010.05.010

Burguière, E., Arleo, A., Hojjati, M. r., Elgersma, Y., De Zeeuw, C. I., Berthoz, A., & Rondi-Reig, L. (2005). Spatial navigation impairment in mice lacking cerebellar LTD: a motor adaptation deficit?. *Nature neuroscience*, *8*(10), 1292–1294. https://doi.org/10.1038/nn1532

Caron, M. J., Mottron, L., Rainville, C., & Chouinard, S. (2004). Do high functioning persons with autism present superior spatial abilities? *Neuropsychologia*, *42*(4), 467–481. https://doi.org/10.1016/j.neuropsychologia.2003.08.015

Chaarani, B., Hahn, S., Allgaier, N., Adise, S., Owens, M. M., Juliano, A. C., Yuan, D. K., Loso, H., Ivanciu, A., Albaugh, M. D., Dumas, J., Mackey, S., Laurent, J., Ivanova, M., Hagler, D. J., Cornejo, M. D., Hatton, S., Agrawal, A., Aguinaldo, L., Ahonen, L., … ABCD Consortium (2021). Baseline brain function in the preadolescents of the ABCD Study. *Nature neuroscience*, *24*(8), 1176–1186. https://doi.org/10.1038/s41593-021-00867-9

Di Martino, A., O'Connor, D., Chen, B., Alaerts, K., Anderson, J. S., Assaf, M., Balsters, J. H., Baxter, L., Beggiato, A., Bernaerts, S., Blanken, L. M. E., Bookheimer, S. Y., Braden, B. B., Byrge,

L., Castellanos, F. X., Dapretto, M., Delorme, R., Fair, D. A., Fishman, I., … Milham, M. P. (2017). Enhancing studies of the connectome in autism using the autism brain imaging data exchange II. *Scientific Data*, *4*, 170010. https://doi.org/10.1038/sdata.2017.10

Dean, S. L., Tochen, L., Augustine, F., Ali, S. F., Crocetti, D., Rajendran, S., Blue, M. E., Mahone, E. M., Mostofsky, S. H., & Singer, H. S. (2022). The Role of the Cerebellum in Repetitive Behavior Across Species: Childhood Stereotypies and Deer Mice. *Cerebellum (London, England)*, *21*(3), 440–451. https://doi.org/10.1007/s12311-021-01301-3

D'Mello, A. M., Crocetti, D., Mostofsky, S. H., & Stoodley, C. J. (2015). Cerebellar gray matter and lobular volumes correlate with core autism symptoms. *NeuroImage : Clinical*, *7*, 631-639. https://doi.org/10.1016/j.nicl.2015.02.007

Fatemi, S. H. (2013). Cerebellum and autism. *Cerebellum (London, England)*, *12*(5), 778-779. https://doi.org/10.1007/s12311-013-0484-9

Fouquet, C., Tobin, C., & Rondi-Reig, L. (2010). A new approach for modeling episodic memory from rodents to humans : The temporal order memory. *Behavioural Brain Research*, *215*(2), 172-179. https://doi.org/10.1016/j.bbr.2010.05.054

Holiga, Š., Hipp, J. F., Chatham, C. H., Garces, P., Spooren, W., D'Ardhuy, X. L., Bertolino, A., Bouquet, C., Buitelaar, J. K., Bours, C., Rausch, A., Oldehinkel, M., Bouvard, M., Amestoy, A., Caralp, M., Gueguen, S., Moal, M. L.-L., Houenou, J., Beckmann, C. F., … Dukart, J. (2019). Patients with autism spectrum disorders display reproducible functional connectivity alterations. *Science Translational Medicine*, *11*(481). https://doi.org/10.1126/scitranslmed.aat9223

Goss-Sampson, M. A. (2020). *Bayesian Inference in JASP*. 1–120. https://doi.org/10.17605/OSF.IO/CKNXM

Igelström, K. M., Webb, T. W., & Graziano, M. S. A. (2017). Functional Connectivity Between the Temporoparietal Cortex and Cerebellum in Autism Spectrum Disorder. *Cerebral Cortex (New York, N.Y.: 1991)*, *27*(4), 2617-2627. https://doi.org/10.1093/cercor/bhw079

Iglói, K., Zaoui, M., Berthoz, A., & Rondi-Reig, L. (2009). Sequential egocentric strategy is acquired as early as allocentric strategy : Parallel acquisition of these two navigation strategies. *Hippocampus*, *19*(12), 1199-1211. https://doi.org/10.1002/hipo.20595

Iglói, K., Doeller, C. F., Berthoz, A., Rondi-Reig, L., & Burgess, N. (2010). Lateralized human hippocampal activity predicts navigation based on sequence or place memory. *Proceedings of*

the National Academy of Sciences of the United States of America, *107*(32), 14466-14471. https://doi.org/10.1073/pnas.1004243107

Iglói, K., Doeller, C. F., Paradis, A.-L., Benchenane, K., Berthoz, A., Burgess, N., & Rondi-Reig, L. (2015). Interaction Between Hippocampus and Cerebellum Crus I in Sequence-Based but not Place-Based Navigation. *Cerebral Cortex (New York, NY)*, *25*(11), 4146-4154. https://doi.org/10.1093/cercor/bhu132

Jeffreys, H. (1961). Theory of probability (3rd ed.). Oxford, UK: Oxford University Press.

Kelly, E., Meng, F., Fujita, H., Morgado, F., Kazemi, Y., Rice, L. C., Ren, C., Escamilla, C. O., Gibson, J. M., Sajadi, S., Pendry, R. J., Tan, T., Ellegood, J., Basson, M. A., Blakely, R. D., Dindot, S. V., Golzio, C., Hahn, M. K., Katsanis, N., … Tsai, P. T. (2020). Regulation of autism-relevant behaviors by cerebellar–prefrontal cortical circuits. *Nature Neuroscience*, *23*(9), 1102-1110. https://doi.org/10.1038/s41593-020-0665-z

Keysers, C., Gazzola, V., & Wagenmakers, E. J. (2020). Using Bayes factor hypothesis testing in neuroscience to establish evidence of absence. *Nature Neuroscience*, 23(7), 788–799. https://doi.org/10.1038/s41593-020-0660-4

Khan, A. J., Nair, A., Keown, C. L., Datko, M. C., Lincoln, A. J., & Müller, R.-A. (2015). Cerebro-cerebellar Resting-State Functional Connectivity in Children and Adolescents with Autism Spectrum Disorder. *Biological Psychiatry*, *78*(9), 625-634. https://doi.org/10.1016/j.biopsych.2015.03.024

Laidi, C., Boisgontier, J., Chakravarty, M. M., Hotier, S., d'Albis, M.-A., Mangin, J.-F. O., Devenyi, G. A., Delorme, R., Bolognani, F., Czech, C., Bouquet, C., Toledano, E., Bouvard, M., Gras, D., Petit, J., Mishchenko, M., Gaman, A., Scheid, I., Leboyer, M., … Houenou, J. (2017). Cerebellar anatomical alterations and attention to eyes in autism. *Scientific Reports*, *7*(1), 12008. https://doi.org/10.1038/s41598-017-11883-w

Lefort, J. M., Vincent, J., Tallot, L., Jarlier, F., De Zeeuw, C. I., Rondi-Reig, L., & Rochefort, C. (2019). Impaired cerebellar Purkinje cell potentiation generates unstable spatial map orientation and inaccurate navigation. *Nature communications*, *10*(1), 2251. https://doi.org/10.1038/s41467-019-09958-5

Lind, S. E., Williams, D. M., Raber, J., Peel, A., & Bowler, D. M. (2013). Spatial Navigation Impairments Among Intellectually High-Functioning Adults With Autism Spectrum Disorder : Exploring Relations With Theory of Mind, Episodic Memory, and Episodic Future Thinking.

Journal of Abnormal Psychology, *122*(4), 1189-1199. https://doi.org/10.1037/a0034819

McGurn, B., Starr, J. M., Topfer, J. A., Pattie, A., Whiteman, M. C., Lemmon, H. A., Whalley, L. J., & Deary, I. J. (2004). Pronunciation of irregular words is preserved in dementia, validating premorbid IQ estimation. *Neurology*, *62*(7), 1184–1186. https://doi.org/10.1212/01.wnl.0000103169.80910.8b

Nelson, H. E. (1982). National Adult Reading Test (NART): For the assessment of premorbid intelligence in patients with dementia: Test manual. Windsor: NFER-Nelson.

Olton, D. S., Samuelson, R.J. (1976) Remembrance of places passed: Spatial memory in rats. J Exp Psychol Anim Behav Process, 2(2), 97-116. https://doi.org/10.1037/0097-7403.2.2.97

Palombi, T., Mandolesi, L., Alivernini, F., Chirico, A., & Lucidi, F. (2022). Application of Real and Virtual Radial Arm Maze Task in Human. Brain Sciences, 12(4), 468. https://doi.org/10.3390/brainsci12040468

Petrosini, L., Leggio, M. G., & Molinari, M. (1998). The cerebellum in the spatial problem solving: a co-star or a guest star?. *Progress in neurobiology*, *56*(2), 191–210. https://doi.org/10.1016/s0301-0082(98)00036-7

Rendall, A. R., Truong, D. T., & Fitch, R. H. (2016). Learning delays in a mouse model of autism spectrum disorder. Behavioural brain research, 303, 201-207. https://doi.org/10.1016/j.bbr.2016.02.006

Ring, M., Gaigg, S. B., Altgassen, M., Barr, P., & Bowler, D. M. (2018). Allocentric Versus Egocentric Spatial Memory in Adults with Autism Spectrum Disorder. *Journal of autism and developmental disorders*, *48*(6), 2101–2111. https://doi.org/10.1007/s10803-018-3465-5

Rochefort, C., Arabo, A., André, M., Poucet, B., Save, E., & Rondi-Reig, L. (2011). Cerebellum shapes hippocampal spatial code. *Science (New York, N.Y.)*, *334*(6054), 385-389. https://doi.org/10.1126/science.1207403

Rondi-Reig, L., & Burguière, E. (2005). Is the cerebellum ready for navigation?. *Progress in brain research*, *148*, 199–212. https://doi.org/10.1016/S0079-6123(04)48017-0

Rondi-Reig, L., Petit, G. H., Tobin, C., Tonegawa, S., Mariani, J., & Berthoz, A. (2006). Impaired sequential egocentric and allocentric memories in forebrain-specific-NMDA receptor knock-out mice during a new task dissociating strategies of navigation. *The Journal of neuroscience: the official journal of the Society for Neuroscience*, *26*(15), 4071–4081. https://doi.org/10.1523/JNEUROSCI.3408-05.2006

Rondi-Reig, L., Paradis, A.-L., Lefort, J. M., Babayan, B. M., & Tobin, C. (2014). How the cerebellum may monitor sensory information for spatial representation. Frontiers in Systems

Neuroscience, 8(Nov), 205. https://doi.org/10.3389/fnsys.2014.00205

Schmahmann, J. D. (1998). Dysmetria of thought : Clinical consequences of cerebellar dysfunction on cognition and affect. *Trends in Cognitive Sciences*, *2*(9), 362-371. https://doi.org/10.1016/S1364-6613(98)01218-2

Schmahmann, J. D., & Caplan, D. (2006). Cognition, emotion and the cerebellum. *Brain*, *129*(2), 290-292. https://doi.org/10.1093/brain/awh729

Sereno, M. I., Diedrichsen, J., Tachrount, M., Testa-Silva, G., d'Arceuil, H., & De Zeeuw, C. (2020). The human cerebellum has almost 80% of the surface area of the neocortex. *Proceedings of the National Academy of Sciences*, *117*(32), 19538-19543. https://doi.org/10.1073/pnas.2002896117

Smith, A. D. (2015). Spatial navigation in autism spectrum disorders : A critical review. *Frontiers in Psychology*, *6*. https://doi.org/10.3389/fpsyg.2015.00031

Stoodley, C. J., Valera, E. M., & Schmahmann, J. D. (2012). Functional topography of the cerebellum for motor and cognitive tasks : An fMRI study. NeuroImage, *59*(2), 1560-1570. https://doi.org/10.1016/j.neuroimage.2011.08.065

Stoodley, C. J., D'Mello, A. M., Ellegood, J., Jakkamsetti, V., Liu, P., Nebel, M. B., Gibson, J. M., Kelly, E., Meng, F., Cano, C. A., Pascual, J. M., Mostofsky, S. H., Lerch, J. P., & Tsai, P. T. (2017). Altered cerebellar connectivity in autism and cerebellar-mediated rescue of autism-related behaviors in mice. *Nature Neuroscience*, *20*(12), 1744-1751. https://doi.org/10.1038/s41593-017-0004-1

Tavor, I., Jones, O. P., Mars, R. B., Smith, S. M., Behrens, T. E., & Jbabdi, S. (2016). Task-free MRI predicts individual differences in brain activity during task performance. *Science*, *352*(6282), 216-220. https://doi.org/10.1126/science.aad8127

Traut, N., Beggiato, A., Bourgeron, T., Delorme, R., Rondi-Reig, L., Paradis, A.-L., & Toro, R. (2018). Cerebellar Volume in Autism : Literature Meta-analysis and Analysis of the Autism Brain Imaging Data Exchange Cohort. *Biological Psychiatry, 83*(7), 579–588. https://doi.org/10.1016/j.biopsych.2017.09.029

van der Kuil, M. N. A., Evers, A. W. M., Visser-Meily, J. M. A., & van der Ham, I. J. M. (2020). The Effectiveness of Home-Based Training Software Designed to Influence Strategic Navigation Preferences in Healthy Subjects. *Frontiers in Human Neuroscience*, *14*.

https://doi.org/10.3389/fnhum.2020.00076

Van Overwalle, F., Baetens, K., Mariën, P., & Vandekerckhove, M. (2014). Social cognition and the cerebellum: a meta-analysis of over 350 fMRI studies. *NeuroImage*, *86*, 554–572. https://doi.org/10.1016/j.neuroimage.2013.09.033

Van Overwalle, F., D'aes, T., & Mariën, P. (2015). Social cognition and the cerebellum: A meta-analytic connectivity analysis. *Human brain mapping*, *36*(12), 5137–5154. https://doi.org/10.1002/hbm.23002

Wang, S. S.-H., Kloth, A. D., & Badura, A. (2014). The cerebellum, sensitive periods, and autism. *Neuron*, *83*(3), 518-532. https://doi.org/10.1016/j.neuron.2014.07.016

Table 1: Details of participants included in the behavioral analysis

	ASD (n = 28)	*TD (n = 31)*	*Test*	BF_{01}	*Interpretation*
Mean age (sd)	31.88 (9.27)	29.34 (7.59)	Mann-Whitney U test	2.22	No difference (anecdotal)
Sex – Males	75%	61%	Chi-square	1.27	Inconclusive
Total IQ (sd)	110 (22)*	NA**			
*Laterality*** - right-handed*	85%	83%	Chi-square	18.18	No difference (strong)
Level of Education (sd)	2.07 (2.89)	3.77 (2.08)	Mann-Whitney U test	0.52	Inconclusive
Exploration speed (sd)	8.58 (2.22)	8.46 (1.81)	Mann-Whitney U test	3.67	No difference (moderate)
Allocentric success	36%	42%	Chi-square	2.90	No difference (anecdotal)
Egocentric success	79%	74%	Chi-square	3.46	No difference (moderate)

ASD: autism spectrum disorder; TD: typical development

* Though data missing for 10 individuals with ASD, global IQ > 70 or IQ > 85 (−1 DS) assessed with the Kaufman Brief Intelligence Test-2 (KBIT2) and the National Adult Reading Test (NART; Nelson, 1982) in Créteil (France).

**NA: Not Available, but global IQ > 70 or IQ > 85 (−1 DS) assessed with the KBIT2 and NART. According to McGurn et al. (2004), NART scores correlate well with IQ to be used as a proxy for premorbid intelligence, and therefore suitable for the assessment of TD individuals. Mean (sd) = 109 (15). See also the similar results of the attentional assessment for ASD and TD groups, in Supplementary Material S7.

*** Data missing for 1 ASD and 1 TD.

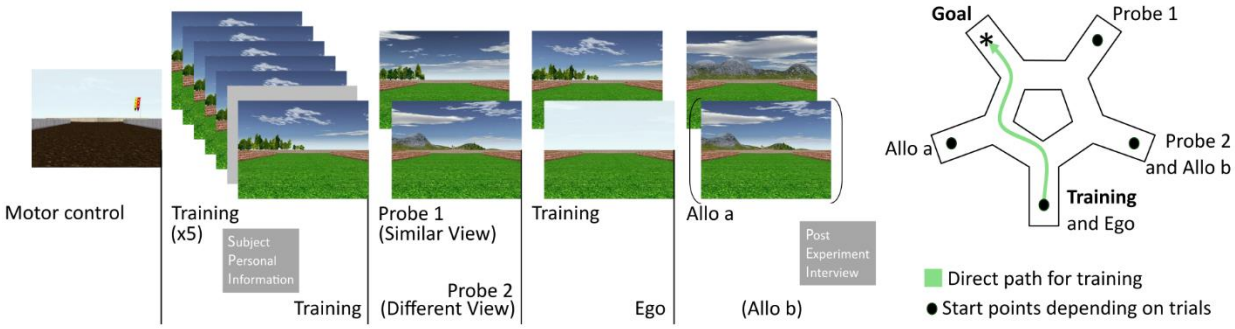

Figure 1. Starmaze procedure. All the participants underwent the following succession of trials: one motor control, five training trials, a break during which participants' personal information was collected, a sixth training trial to assess recall after the break, two probe tests with a view at the departure point either similar or different from the view at the start of the training trials, and the last training trial just before the trials designed to force the use of the sequence-based strategy (Ego trial) and place-based strategy (Allo a and b trials). The Allo b trial was performed by only part of the participants and therefore not analyzed in this study. The procedure ended with a post-experiment interview. The right panel illustrates the location of the goal (*) and the different departure points depending on the trials. The green arrow shows the shortest way from the usual training departure to the goal (direct path), which passes through four alleys (2 peripheral and 2 central) and requires three turns (left-right-left).

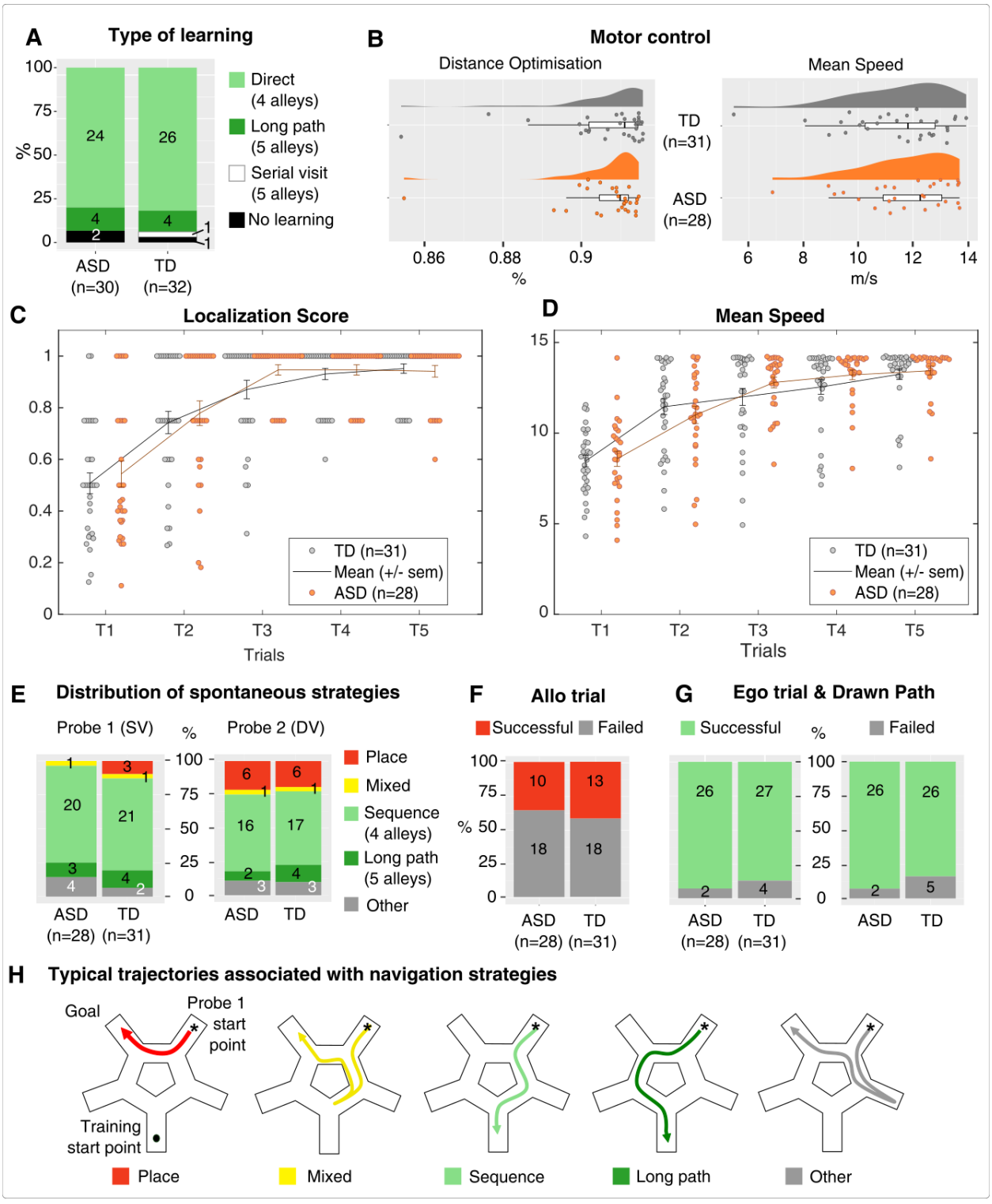

Figure 2. Learning of the Starmaze task across individuals with ASD and TD. (A) Participants' learning strategies used at least twice between training trials 4 and 6 separately for each group. The following scores (B-H) were only computed for the participants who learned

the task. (B) Distribution of motor-control parameters (Distance optimization and Mean speed) per group. (C-D) Learning curves per group across the first five trainings for the localization score and the mean traveling speed, respectively. (E) Distribution of spontaneous strategies used by individuals with ASD and TD during Probe1 (SV: departure point with Similar View as training) or Probe 2 (DV: departure point with Different View from training). (F) Proportion of successful participants per group at the Allo trial. (G) Proportion of participants successful at the Ego trial (left side) and at reproducing on a Starmaze schema their own preferred path (Drawn path, right side). (H) Schematic representation of the six different strategies used by participants during the probe trials. ASD: autism spectrum disorder; TD: typical development.

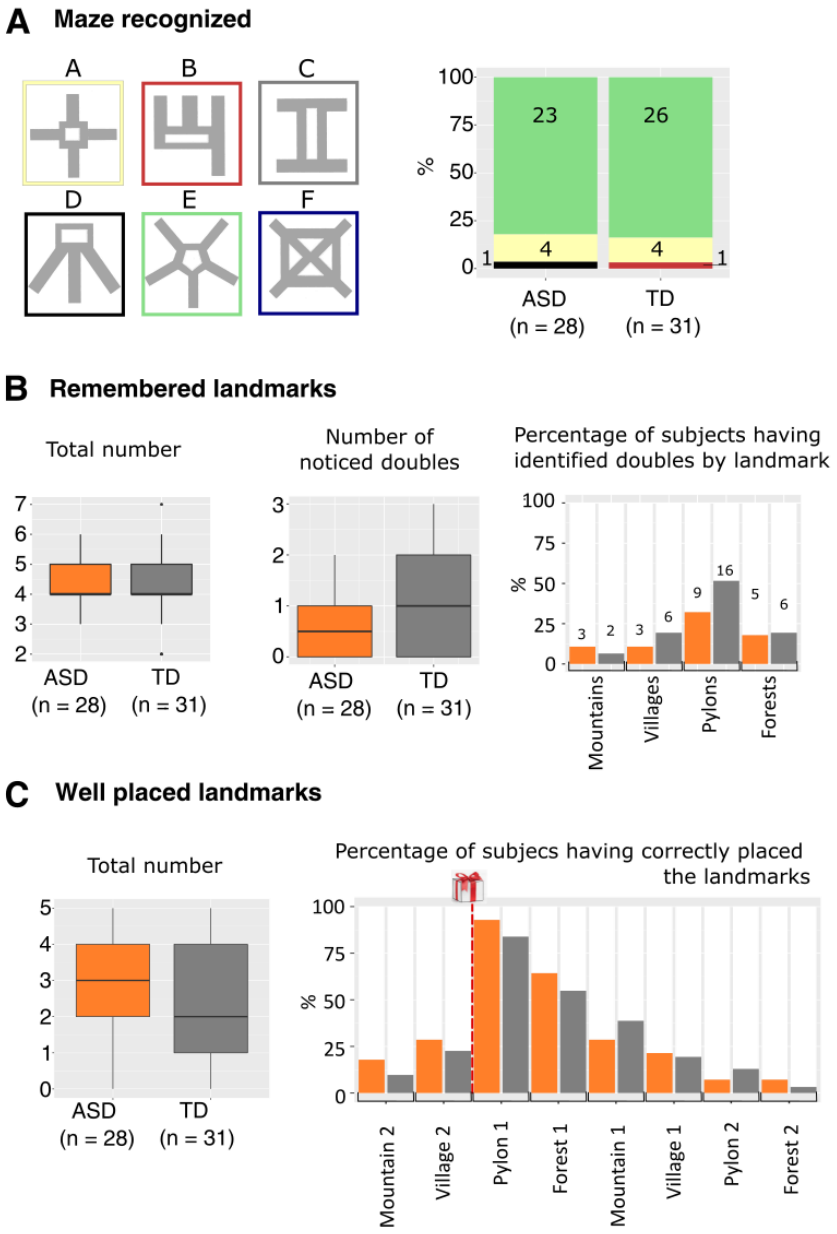

Figure 3: Internal representation of the virtual environment after task learning. (A) Different shapes among which the participants had to recognize the maze in which they had performed the navigation task and percentage of participants having designated each form. (B) From left to right, total number of landmarks memorized by participants out of eight possible, total number of doubles noticed out of four possible, and percentage of individuals who identified doubles for each type of landmark. (C) Total number of memorized landmarks that were correctly placed around the maze map per participant, and percentage of individuals who correctly placed each of the landmarks.

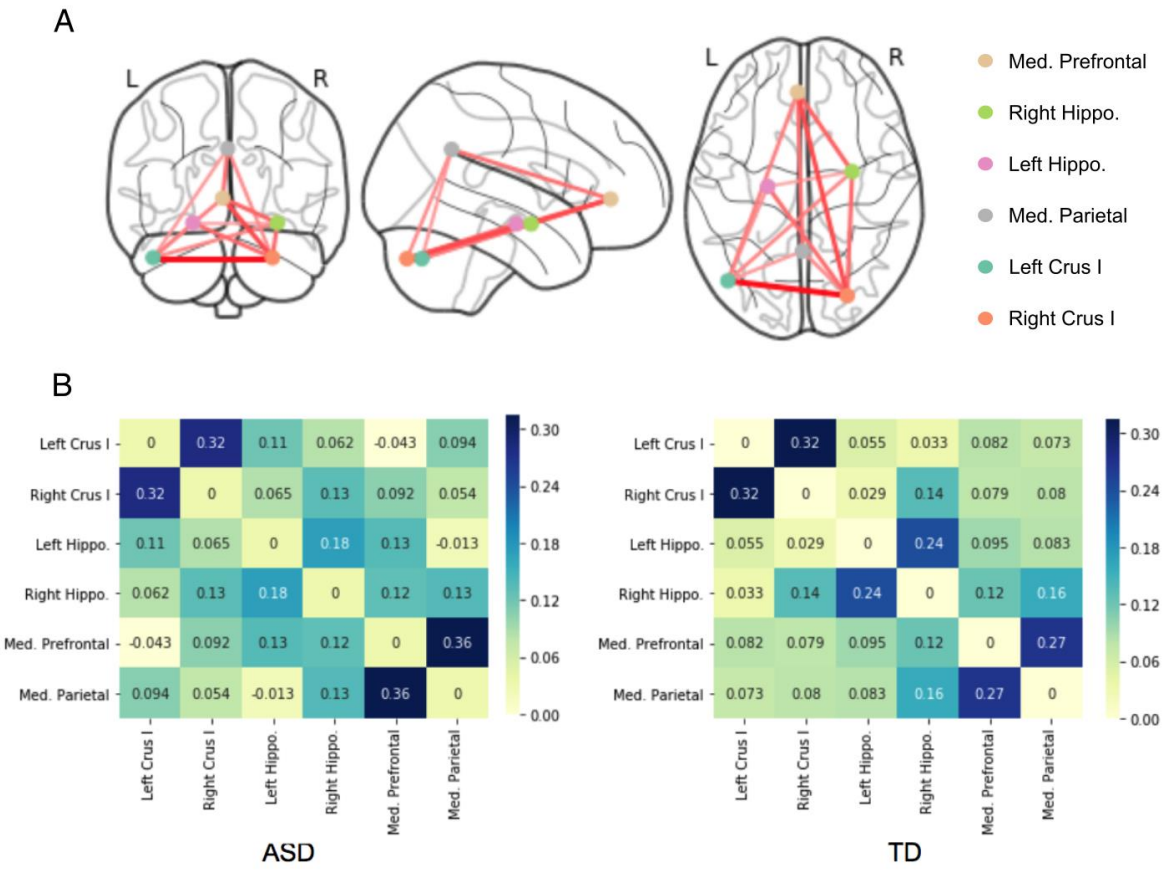

Figure 4: Cerebellum, hippocampus, medial parietal, and medial prefrontal functional connectivity. (A) Representation of cerebellar functional connectivity between cerebellum, hippocampus, medial prefrontal and medial parietal cortex on a glass brain. Left Crus I (dark green), Right Crus I (orange), Left hippocampus (purple), Right Hippocampus (light green), Medial parietal cortex (gray), Medial prefrontal cortex (golden); the thickness and color intensity of the in-between segments represent the correlation strength. (B) Correlation matrices between the regions of interest (see A) in the ASD and TD group. Hippo: hippocampus; Med. Prefrontal: medial prefrontal cortex; Med. Parietal: medial parietal cortex. ASD: Individuals with autism spectrum disorder; TD: Individual with typical development.

Supplementary Material S1: Flow chart of the study

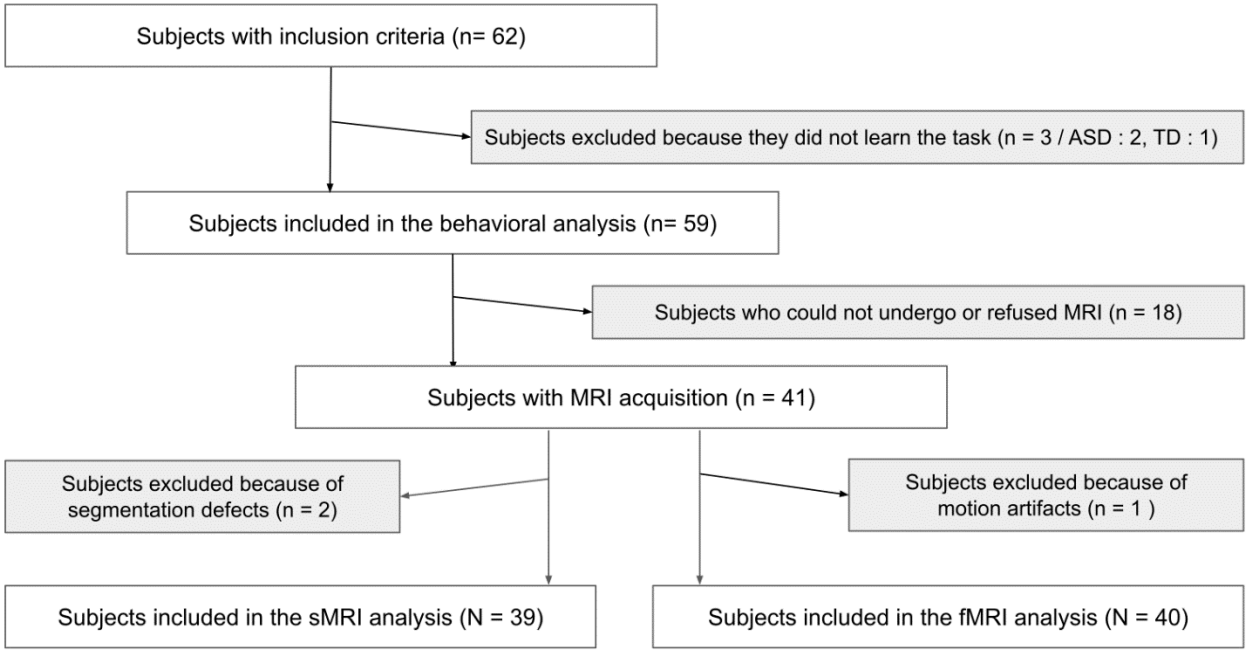

Supplementary Material S2: Methods for the MRI data analysis

S2.a. Navigation scores for MRI data analysis

To test a possible association of the navigation behavior with anatomy and functional connectivity at rest, we selected three scores reflecting three main aspects of navigation:

-The Exploration speed (ExS): Average speed during the first training trial, from the first movement with the joystick (rotation or translation). This speed increases with the amount of physical exploration (forward movements in the maze) and decreases with the time spent staying still in the maze or rotating on oneself to visually explore the environment.

- Allocentric success (Allo, dichotomous variable): This score distinguishes the participants who are able to directly reach the goal in the Allo a trial (Allocentric success = 1) from those failing to reach the goal or using an indirect way to reach it (Allocentric success = 0).

- Egocentric score (Ego, dichotomous variable): This score distinguishes the participants who have both the ability and a tendency to rely on a learned path. The learned path is the one most reproduced among the last 3 learning trials (and which determines the type of learning as seen in Figure 2.A). If the participants perfectly reproduce this learned path 1) in the first probe trial (Probe 1), 2) in the absence of distant visual cues (Ego trial), and 3)by drawing on the paper map, their Egocentric score is 1. The Egocentric score is 0 in all other conditions.

S2.b. Structural MRI acquisition and processing

Participants underwent a T1 weighted MRI (T1) (Supplementary Material S1 – Flow chart) with a full coverage of the cerebellum. All data were acquired with a 3T Siemens Prisma MRI equipped with a standard 12-channel head coil. MR data were obtained using a 3DT1-weighted sequence (voxel size = 1 x 1 mm, slice thickness = 1.1 mm, TR = 2300 ms, FOV = 256 mm). All T1 images were processed using the CERES pipeline that performs a fully automated segmentation and parcellation of the cerebellum (Romero et al., 2017) (Supplementary Material S2.c) following the protocol described in Park et al.'s paper (Park et al., 2014). Afterwards, we extracted the volume of the Crus I, a region of interest previously involved in spatial navigation (Stoodley et al., 2012 and Igloi et al., 2015). All volumes were visually inspected by an examiner (CL) blind to the diagnosis in order to ensure the quality of the segmentation.

Iglói, K., Doeller, C. F., Paradis, A. L., Benchenane, K., Berthoz, A., Burgess, N., & Rondi-Reig, L. (2015). Interaction Between Hippocampus and Cerebellum Crus I in Sequence-Based but not Place-Based Navigation. *Cerebral cortex (New York, N.Y.: 1991)*, *25*(11), 4146–4154. https://doi.org/10.1093/cercor/bhu132

Park, M. T., Pipitone, J., Baer, L. H., Winterburn, J. L., Shah, Y., Chavez, S., Schira, M. M., Lobaugh, N. J., Lerch, J. P., Voineskos, A. N., & Chakravarty, M. M. (2014). Derivation of high-resolution MRI atlases of the human cerebellum at 3T and segmentation using multiple automatically generated templates. NeuroImage, 95, 217–231. https://doi.org/10.1016/j.neuroimage.2014.03.037

Romero, J. E., Coupé, P., Giraud, R., Ta, V. T., Fonov, V., Park, M., Chakravarty, M. M., Voineskos, A. N., & Manjón, J. V. (2017). CERES: A new cerebellum lobule segmentation method. NeuroImage, 147, 916–924. https://doi.org/10.1016/j.neuroimage.2016.11.003

Stoodley, C. J., Valera, E. M., & Schmahmann, J. D. (2012). Functional topography of the cerebellum for motor and cognitive tasks: an fMRI study. *NeuroImage*, *59*(2), 1560–1570. https://doi.org/10.1016/j.neuroimage.2011.08.065

S2.c. Parcellation of the cerebellum with CERES automated pipeline (https://volbrain.upv.es/)

A. Isolation of the intracranial volume.

B. Automated cerebellar parcellation; black arrow (right Crus I), red arrow (left Crus I)

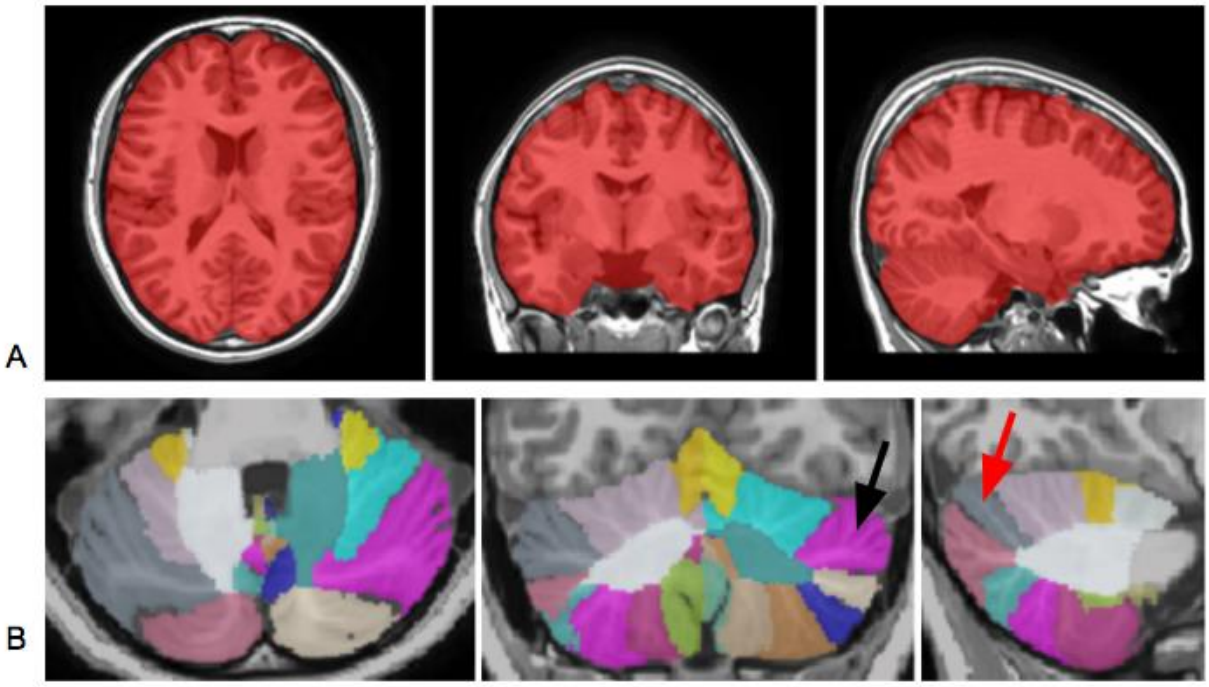

S2.d. Functional MRI acquisition and pre-processing

Participants underwent in addition to the structural MRI a functional MRI sequence (voxel size = 2.5 x 2.5 x 2.5 mm, TR = 1430 ms, TE = 20 ms, multi-band factor accelerator = 2). All images were pre-processed using the fmri prep freely available pipeline (https://fmriprep.readthedocs.io/en/stable/). We performed brain extraction, brain tissue segmentation, spatial normalization, head-motion estimation, susceptibility distortion correction, functional to structural registration. We did not perform slice time correction since we used multi-band acquisition. Functional images were resampled onto standard MNI space and confounds estimation were extracted. We performed an automated quality control of the normalized functional images using the mriqc freely available pipeline (https://mriqc.readthedocs.io/en/stable/). In order to limit the number of tests when studying the cerebellar functional connectivity, we focused our analysis on the cerebro-cerebellar circuits involved in navigation and extracted the time series using nilearn python package

(https://nilearn.github.io/) in the following regions of interest: left and right Crus I, left and right hippocampus, medial parietal and medial prefrontal cortex, based on the coordinates of Igloi et al. (Igloi et al., 2015). We hypothesized, based on our previous work (Igloi et al., 2015), that the cerebellar circuits involved in spatial navigation would be disrupted in individuals with ASD.

S2.e. Quality check and pre-processing of the functional MRI data

Functional MRI (fMRI) data were converted from NIFTI to DICOM (Li et al., 2016), then converted to Brain Imaging Data Structure (BIDS) format, verified using the BIDS validator (http://bids-standard.github.io/bids-validator/). To check the quality of our data, we used MRIQC v0.10.1 (Esteban et al., 2017) to extract Images Quality Metrics (IQMs) and visual reports. Three subjects were excluded because of a mean framewise displacement above a cut-off of 0.3 mm.

Functional MRI pre-processing was performed with fMRIPrep 1.5.0 (Esteban et al., 2018), based on a Nipype 1.2.2 tool (Gorgolewski et al., 2011). The following was generated automatically by fMRIPrep software.

First, a reference volume and its skull-stripped version were generated using a custom methodology of fMRIPrep. The BOLD reference was then co-registered to the T1w reference using flirt (FSL 5.0.9) with the boundary-based registration (Greve and Fischl, 2009) cost-function. Co-registration was configured with nine degrees of freedom to account for distortions remaining in the BOLD reference. Head-motion parameters with respect to the BOLD reference (transformation matrices, and six corresponding rotation and translation parameters) are estimated before any spatiotemporal filtering using mcflirt (FSL 5.0.9, Jenkinson et al. 2002). BOLD runs were slice-time corrected using 3dTshift from AFNI (Cox et al., 1997). The BOLD time-series (including slice-timing correction) were resampled onto their original, native space by applying a single, composite transform to correct for head-motion and susceptibility distortions. These resampled BOLD time-series will be referred to as preprocessed BOLD in original space, or just preprocessed BOLD. The BOLD time-series were resampled into standard space, generating a preprocessed BOLD run in MNI space. First, a reference volume and its skull-stripped version were generated using a custom methodology of fMRIPrep. Several confounding time-series were calculated based on the preprocessed BOLD: framewise displacement (FD), DVARS and three region-wise global signals. FD and DVARS are calculated for each functional run, both using their implementations in Nipype (following the definitions by Power et al., 2014). The three global signals are extracted within the CSF, the WM, and the whole-brain masks. Additionally, a set of physiological regressors were extracted to allow for component-based noise

correction (CompCor, Behzadi et al., 2007). Principal components are estimated after high-pass filtering the preprocessed BOLD time-series (using a discrete cosine filter with 128s cut-off) for the two CompCor variants: temporal (tCompCor) and anatomical (aCompCor). tCompCor components are then calculated from the top 5% variable voxels within a mask covering the subcortical regions. This subcortical mask is obtained by heavily eroding the brain mask, which ensures it does not include cortical GM regions. For aCompCor, components are calculated within the intersection of the aforementioned mask and the union of CSF and WM masks calculated in T1w space, after their projection to the native space of each functional run (using the inverse BOLD-to-T1w transformation). Components are also calculated separately within the WM and CSF masks. For each CompCor decomposition, the k components with the largest singular values are retained, such that the retained components' time series are sufficient to explain 50 percent of variance across the nuisance mask (CSF, WM, combined, or temporal). The remaining components are dropped from consideration. The head-motion estimates calculated in the correction step were also placed within the corresponding confounds file. The confound time series derived from head motion estimates and global signals were expanded with the inclusion of temporal derivatives and quadratic terms for each (Satterthwaite et al., 2013). Frames that exceeded a threshold of 0.5 mm FD or 1.5 standardised DVARS were annotated as motion outliers. All resamplings can be performed with a single interpolation step by composing all the pertinent transformations (i.e. head-motion transform matrices, susceptibility distortion correction when available, and co-registrations to anatomical and output spaces). Gridded (volumetric) resamplings were performed using antsApplyTransforms (ANTs), configured with Lanczos interpolation to minimize the smoothing effects of other kernels (Lanczos, 1964). Non-gridded (surface) resamplings were performed using mri_vol2surf (FreeSurfer). Many internal operations of fMRIPrep use Nilearn 0.5.2 (Abraham et al., 2014, RRID:SCR_001362), mostly within the functional processing workflow. For more details of the pipeline, see the section corresponding to workflows in fMRIPrep's documentation.

Abraham, A., Pedregosa, F., Eickenberg, M., Gervais, P., Mueller, A., Kossaifi, J., Gramfort, A., Thirion, B., & Varoquaux, G. (2014). Machine learning for neuroimaging with scikit-learn. *Frontiers in neuroinformatics*, *8*, 14. https://doi.org/10.3389/fninf.2014.00014

Behzadi, Y., Restom, K., Liau, J., & Liu, T. T. (2007). A component based noise correction method (CompCor) for BOLD and perfusion based fMRI. *NeuroImage*, *37*(1), 90–101. https://doi.org/10.1016/j.neuroimage.2007.04.042

Cox, R. W., & Hyde, J. S. (1997). Software tools for analysis and visualization of fMRI data. *NMR*

in biomedicine, *10*(4-5), 171–178. https://doi.org/10.1002/(sici)1099-1492(199706/08)10:4/5<171::aid-nbm453>3.0.co;2-l

Esteban, O., Birman, D., Schaer, M., Koyejo, O. O., Poldrack, R. A., & Gorgolewski, K. J. (2017). MRIQC: Advancing the automatic prediction of image quality in MRI from unseen sites. *PloS one*, 12(9), e0184661. https://doi.org/10.1371/journal.pone.0184661

Esteban, O., Markiewicz, C. J., Blair, R. W., Moodie, C. A., Isik, A. I., Erramuzpe, A., Kent, J. D., Goncalves, M., DuPre, E., Snyder, M., Oya, H., Ghosh, S. S., Wright, J., Durnez, J., Poldrack, R. A., & Gorgolewski, K. J. (2019). fMRIPrep: a robust preprocessing pipeline for functional MRI. Nature methods, 16(1), 111–116. https://doi.org/10.1038/s41592-018-0235-4

Gorgolewski, K., Burns, C. D., Madison, C., Clark, D., Halchenko, Y. O., Waskom, M. L., & Ghosh, S. S. (2011). Nipype: a flexible, lightweight and extensible neuroimaging data processing framework in python. *Frontiers in neuroinformatics*, *5*, 13. https://doi.org/10.3389/fninf.2011.00013

Greve, D. N., & Fischl, B. (2009). Accurate and robust brain image alignment using boundary-based registration. *NeuroImage*, *48*(1), 63–72. https://doi.org/10.1016/j.neuroimage.2009.06.060

Jenkinson, M., Bannister, P., Brady, M., & Smith, S. (2002). Improved optimization for the robust and accurate linear registration and motion correction of brain images. *NeuroImage*, *17*(2), 825–841. https://doi.org/10.1016/s1053-8119(02)91132-8

Lanczos, C. (1964). Evaluation of Noisy Data. *Journal of the Society for Industrial and Applied Mathematics Series B Numerical Analysis* 1 (1): 76–85. https://doi.org/10.1137/0701007.

Li, X., Morgan, P. S., Ashburner, J., Smith, J., & Rorden, C. (2016). The first step for neuroimaging data analysis: DICOM to NIfTI conversion. *Journal of neuroscience methods*, 264, 47–56. https://doi.org/10.1016/j.jneumeth.2016.03.001

Power, J. D., Mitra, A., Laumann, T. O., Snyder, A. Z., Schlaggar, B. L., & Petersen, S. E. (2014). Methods to detect, characterize, and remove motion artifact in resting state fMRI. *NeuroImage*, *84*, 320–341. https://doi.org/10.1016/j.neuroimage.2013.08.048

Satterthwaite, T. D., Elliott, M. A., Gerraty, R. T., Ruparel, K., Loughead, J., Calkins, M. E., Eickhoff, S. B., Hakonarson, H., Gur, R. C., Gur, R. E., & Wolf, D. H. (2013). An improved framework for confound regression and filtering for control of motion artifact in the preprocessing of resting-state functional connectivity data. *NeuroImage*, 64, 240–256.

https://doi.org/10.1016/j.neuroimage.2012.08.052

S2.f. Frequentist statistical analyses for MRI data

We tested the normality of the distribution of continuous variables with the omnibus test for normality (scipy.stats.normaltest function in Python's statsmodel package - https://www.statsmodels.org). If the distribution was normal, we compared both groups (ASD and neurotypical individuals) with student t-tests. We compared categorical variables with chi-2 tests or exact Fisher tests if the conditions for the chi-2 test were not fulfilled. To assess the learning phase we performed a two-ways linear mixed model with factors Trial (1 to 5) and Group (ASD/TD).

In order to estimate how diagnosis and navigation strategies were associated with Crus I volume, we fitted a linear model with Crus I volume as a dependent variable and age, sex, intracranial volume, diagnosis group (ASD or TD) and navigation score as covariates. We fitted three linear models for each navigation score (ExS, Ego, Allo). In addition, for each navigation strategy, we tested a diagnostic by navigation strategy interaction. Before performing pairwise comparisons (t-tests), we ensured that the standardized residuals were normally distributed, as assessed by the Shapiro–Wilk test ($P > 0.05$) and a QQ-plot. We applied a false discovery rate correction (FDR – Benjamini Hochberg correction) to control multiple testing.

We computed Spearman correlation between the six time series extracted from our regions of interest. Next, we tested the association between selected correlations, navigation scores and the diagnostic group, by fitting linear models including the correlation as a dependent variable and age, sex, mean framework displacement (mean FD), navigation score and diagnosis group (ASD or TD) as covariates. In addition, for each navigation score, we tested a diagnosis by navigation score interaction. Before performing pairwise comparisons (t-tests), we ensured that the standardized residuals were normally distributed, as assessed by the Shapiro–Wilk test ($P > 0.05$) and a QQ-plot. We applied a false discovery rate correction (FDR – Benjamini Hochberg correction) to control for multiple testing.

S2.g. Participants included in the structural MRI analysis

	ASD (n = 17)	***TD (n = 22)***	***Test***	***BF_{01}***	***Interpretation***
Mean age (sd)	32.09 (9.40)	29.77 (8.33)	Mann-Whitney U test	2.43	No difference (anecdotal)
Sex – Males	82%	54%	Chi^2	0.56	Inconclusive
Laterality - right-handed	88%	81% *	Chi^2	10.90	No difference (strong)
Level of Education (sd)	1.41 (3.02)	3.91 (2.00)	Mann-Whitney U test	0.36	Difference (anecdotal)
Exploration speed (sd)	8.74 (2.19)	8.25 (1.72)	Mann-Whitney U test	2.46	No difference (anecdotal)
Allocentric success	29%	36%	Chi^2	2.52	No difference (anecdotal)
Egocentric success	82%	73%	Chi^2	2.48	No difference (anecdotal)

*ASD: autism spectrum disorder; TD: typical development; * TD (n=21)*

S2.h. Participants included in the functional MRI analysis

	ASD (n = 16)	***TD (n = 24)***	***Test***	***BF_{01}***	***Interpretation***
Mean age (sd)	31.31 (9.79)	29.35 (8.11)	Mann-Whitney U test	2.74	No difference (anecdotal)
Sex – Males	88%	54%	Chi^2	0.26	Difference (moderate)
Laterality - right-handed	81%	83%	Chi^2	10.31	No difference (strong)
Level of Education (sd)	1.50 (2.83)	3.96 (1.92)	Mann-Whitney U test	0.29	Difference (moderate)
Exploration speed (sd)	8.61 (2.22)	8.34 (1.69)	Mann-Whitney U test	2.90	No difference (anecdotal)
Allocentric success	31%	38%	Chi^2	2.55	No difference (anecdotal)
Egocentric success	81%	75%	Chi^2	2.86	No difference (anecdotal)

ASD: autism spectrum disorder; TD: typical development

Supplementary Material S3: No association between cerebellar Crus I volume, diagnosis and navigation strategies

S3.a. Bayesian Statistics

The columns report the contribution of each factor (age, sex, ICV, diagnosis, nav. score, and interactions) to the volume of Crus I, after the results of a Bayesian ANCOVA. ICV: intracranial volume; Nav.: navigation.

Tested region →	Bilateral Crus I		Right Crus I		Left Crus I	
Nav. Score →	Exploration speed [a]		Egocentric score [b]		Allocentric success [c]	
	BF_{excl}	Contribution (evidence)	BF_{excl}	Contribution (evidence)	BF_{excl}	Contribution (evidence)
Age	0.664	Inconclusive	0.987	Inconclusive	1.653	Inconclusive
Sex	2.228	No (anecdotal)	2.368	No (anecdotal)	2.386	No (anecdotal)
ICV	0.002	Yes (extreme)	0.016	Yes (extreme)	0.003	Yes (extreme)
Diagnosis	2.483	No (anecdotal)	2.895	No (anecdotal)	2.891	No (anecdotal)
Sex * Diagnosis	2.003	No (anecdotal)	1.919	Inconclusive	1.774	Inconclusive
Nav. score	0.462	Yes (anecdotal)	2.084	No (anecdotal)	1.858	Inconclusive
Sex * Nav. Score	-		1.799	Inconclusive	1.591	Inconclusive
Diagnosis * Nav. score	2.971	No (anecdotal)	2.124	No (anecdotal)	1.893	Inconclusive
Sex * Diagnosis * Nav. score	-		1.297	Inconclusive	1.697	Inconclusive

a: factors = Sex + Diagnosis; covariates: Age + ICV + Exploration speed + Exploration speed*Diagnosis;

b: factors = Sex + Diagnosis + Egocentric score; covariate: Age + ICV;

c: factors = Sex + Diagnosis + Allocentric success; covariates: Age + ICV ;

S3.b. Frequentist statistics

The columns report the impact of each factor (age, sex, ICV, diagnosis, navigation score, and diagnosis x navigation score) on the volume of Crus I, after the results of a linear model. ICV: intracranial volume

Navigation score ->	Exploration speed [a]		Egocentric score [b]		Allocentric success [c]	
	t-stat	pval	t-stat	pval	t-stat	pval
Age	- 2.4	0.023 *	- 1.87	0.07	- 1.7	0.085
Sex	- 0.47	0.64	0.35	0.73	0.069	0.95
ICV	3.7	0.001 *	3.72	0.001 *	3.2	0.003 *
Diagnosis	0.7	0.49	0.23	0.82	1.2	0.24
Navigation score	- 1.29	0.21	0.01	0.99	0.63	0.53
Diagnosis * Navigation score	- 0.76	0.46	- 0.24	0.81	- 1.24	0.24

*: p value < 0.05

a: results for the linear model: Crus I volume = age + sex + ICV + diagnosis + exploration speed + interaction (diagnosis * exploration speed)

b: results for the linear model: Crus I volume = age + sex + ICV + diagnosis + egocentric score + interaction (diagnosis * egocentric score)

c: results for the linear model: Crus I volume = age + sex + ICV + diagnosis + allocentric success + interaction (diagnosis * allocentric success)

S3.c. No difference between ASD and TD in Crus I grey matter volume

Blue (TD, n = 22) and orange (ASD, n = 17) dots represent the standardized residuals of a linear model, after regressing out the effect of age, intracranial volume and sex. ASD: autism spectrum disorder; TD: typical development.

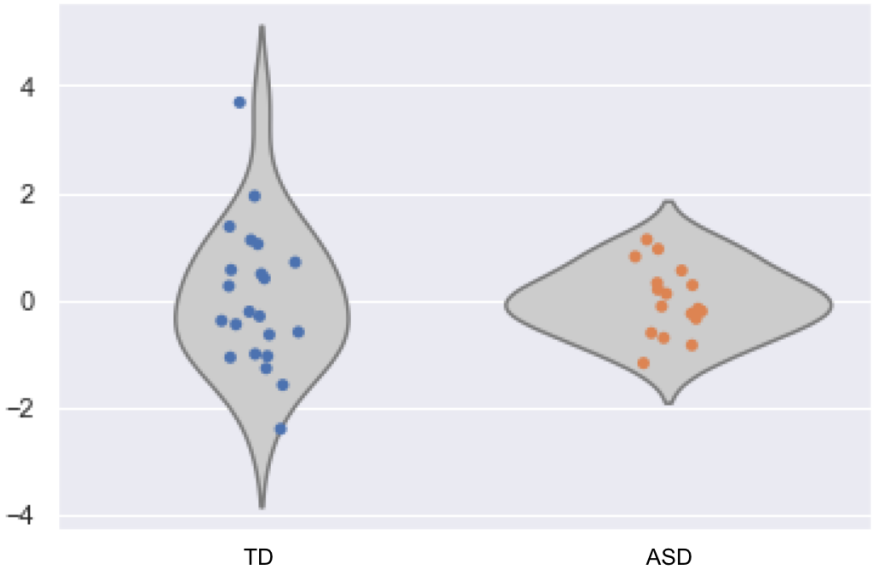

Supplementary Material S4: No Association between navigation scores, diagnosis and Cerebro-cerebellar connectivity

S4.a. Bayesian statistics

The columns report the contribution of each factor (age, Mean FD, sex, diagnosis, navigation score, and interactions) in the correlation of activity between specific structure couples, after the results of a bayesian ANCOVA. In grey, inconclusive results (1/2<BFexcl<2); In black, anecdotal to moderate evidence of an absence of contribution (2<BFexcl<3). FD: framework displacement; Nav.: navigation; hippo.: hippocampus; PFC: prefrontal cortex

Navigation score ->	**Exploration speed [a]**			**Egocentric score [b]**		**Allocentric success [b]**
Resting-state functional connectivity	**Left Crus I - Parietal cortex**	**Right Crus I - Left hippo.**	**Right Crus I - medial PFC**	**Right Crus I - Left hippo.**	**Right Crus I - medial PFC**	**Left Crus I - Parietal cortex**
Age	1.717	0.797	0.872	0.896	1.209	1.716
Mean FD	1.086	2.265	1.559	2.626	1.910	1.098
Sex	3.010	2.985	2.933	2.998	2.953	2.580
Diagnosis	2.464	1.496	1.685	1.637	1.923	2.913
Diagnosis * Nav. score	1.667	1.638	1.733	1.258	1.724	2.203

a: factors = Sex + Diagnosis; covariates: Age + Mean FD + Explo. speed + Explo. speed*Diagnosis;

b: factors = Sex + Diagnosis + Allocentric success; covariates: Age + Mean FD;

c: factors = Diagnosis + Egocentric score; covariates: Age + Mean FD + Sex.

S4.b. Frequentist statistics

The columns report the impact of each factor (age, Mean FD, sex, diagnosis, navigation score, and diagnosis x navigation score interaction) on the correlation of activity between specific structure couples. FD: framework displacement; Nav.: navigation; hippo.: hippocampus; PFC: prefrontal cortex

Nav. score →	**Exploration speed**			**Egocentric score**		**Allocentric success**
Resting-state functional connectivity	**Left Crus I - Parietal cortex**	**Right Crus I - Left hippo.**	**Right Crus I - medial PFC**	**Right Crus I - Left hippo.**	**Right Crus I - medial PFC**	**Left Crus I - Parietal cortex**
Age (t stat / pval)	- 1.3 / 0.22	- 1.46 / 0.16	- 1.22 / 0.27	**-2.14 /0.040**	- 1.30 / 0.21	- 1.49 / 0.145
Mean FD (t stat / pval)	- 0.87 / 0.40	1.46 / 0.156	0.78 / 0.44	1.80 / 0.08	- 0.34 / 0.73	- 0.37 / 0.71
Sex (t stat / pval)	0.065 / 0.95	0.076 / 0.94	0.54 / 0.59	0.41 / 0.70	0.39 / 0.70	0.97 / 0.34
Diagnosis (t stat / pval)	1.50 / 0.14	0.065 / 0.95	0.047 / 0.96	- 0.50 / 0.62	0.36 / 0.72	1.33 / 0.19
Diagnosis * Nav. score (t stat / pval)	- 1.48 / 0.15	- 0.039 / 0.969	0.032 / 0.98	- 0.78 / 0.44	- 0.58 / 0.57	- 1.36 / 0.18

Supplementary Material S5: Results of frequentist statistical analyses for behavioral data

S5.a. Navigation data reported in Figure 2

A_Type of learning

Comparison of direct path proportions

		95% Confidence Intervals		
	Log Odds Ratio	**Lower**	**Upper**	**p**
Odds ratio	-0.080	-1.340	1.180	
Fisher's exact test	-0.079	-1.541	1.382	1.000

B_Motor control

Independent Samples Mann-Whitney U test				**95% CI for Rank-Biserial Correlation**	
	W	***p***	**Rank-Biserial Correlation**	**Lower**	**Upper**
Distance Optimization	362.00	*0.280*	-0.166	-0.434	0.129
Mean speed	478.00	*0.512*	0.101	-0.193	0.379

Note. For the Mann-Whitney test, effect size is given by the rank biserial correlation.

C_Training Phase - Localization score

ANOVA (correction for non-parametric testing)

Cases	**Sum of Squares**	**df**	**Mean Square**	**F**	**p**	**η^2**
Group	0.069	1	0.069	2.002	0.158	0.004
Trial	7.532	4	1.883	54.523	< .001	0.430
Group ✻ Trial	0.059	4	0.015	0.429	0.787	0.003
Residuals	9.842	285	0.035			

Note. Type III Sum of Squares

Post Hoc Comparisons for Localization score - Trial

			95% CI for Mean Difference					
		Mean Difference	Lower	Upper	SE	t	Cohen's d	p_{bonf}
1	2	-0.235	-0.329	-0.141	0.034	-6.864	-0.958	*< .001*
	3	-0.383	-0.477	-0.289	0.034	-11.177	-1.839	*< .001*
	4	-0.413	-0.507	-0.319	0.034	-12.056	-2.164	*< .001*
	5	-0.421	-0.515	-0.327	0.034	-12.283	-2.223	*< .001*
2	3	-0.148	-0.242	-0.054	0.034	-4.313	-0.707	*< .001*
	4	-0.178	-0.272	-0.084	0.034	-5.192	-0.928	*< .001*
	5	-0.186	-0.280	-0.092	0.034	-5.419	-0.976	*< .001*
3	4	-0.030	-0.124	0.064	0.034	-0.879	-0.214	*1.000*
	5	-0.038	-0.132	0.056	0.034	-1.106	-0.273	*1.000*
4	5	-0.008	-0.102	0.086	0.034	-0.228	-0.070	*1.000*

Note. Cohen's d does not correct for multiple comparisons.
Note. P-value and confidence intervals adjusted for comparing a family of 5 estimates (confidence intervals corrected using the Tukey method).

D_Training Phase – Mean Speed

ANOVA (correction for non-parametric testing)

Cases	Sum of Squares	df	Mean Square	F	p	η^2
Group	5.093	1	5.093	1.228	0.269	0.002
Trial	876.760	4	219.190	52.835	< .001	0.422
Group ✻ Trial	14.407	4	3.602	0.868	0.483	0.007
Residuals	1182.337	285	4.149			

Note. Type III Sum of Squares

Post Hoc Comparisons For Mean Speed - Trial

			95% CI for Mean Difference					
		Mean Difference	Lower	Upper	SE	t	Cohen's d	p_{bonf}
1	2	-2.708	-3.739	-1.677	0.375	-7.212	-1.207	< .001
	3	-3.874	-4.905	-2.843	0.375	-10.317	-1.846	< .001
	4	-4.357	-5.388	-3.326	0.375	-11.604	-2.228	< .001
	5	-4.823	-5.854	-3.792	0.375	-12.845	-2.738	< .001
2	3	-1.166	-2.197	-0.135	0.375	-3.105	-0.500	0.021
	4	-1.649	-2.680	-0.618	0.375	-4.392	-0.748	< .001
	5	-2.115	-3.146	-1.084	0.375	-5.633	-1.040	< .001
3	4	-0.483	-1.514	0.548	0.375	-1.287	-0.235	1.000
	5	-0.949	-1.980	0.082	0.375	-2.528	-0.507	0.120
4	5	-0.466	-1.497	0.565	0.375	-1.241	-0.273	1.000

Note. Cohen's d does not correct for multiple comparisons.
Note. P-value and confidence intervals adjusted for comparing a family of 5 estimates (confidenc intervals corrected using the Tukey method).
Note. Results are averaged over the levels of: group

E_Distribution of spontaneous strategies

Comparison of strategy distribution in Probes, and success rate in Allo trial, Ego trial and path drawing

			95% Confidence Intervals		
		Log Odds Ratio	Lower	Upper	p
Probe 1: Visual vs. Sequence	Odds ratio	1.303	-0.960	3.566	
	Fisher's exact test	1.281	-1.125	5.241	0.362
Probe 2: Visual vs. Sequence	Odds ratio	-0.154	-1.376	1.068	
	Fisher's exact test	-0.151	-1.555	1.250	1.000
Probe 1: Extended visual vs. Sequence	Odds ratio	0.099	-1.216	1.414	
	Fisher's exact test	0.097	-1.417	1.656	1.000
Probe 2: Extended visual vs. Sequence	Odds ratio	-0.154	-1.233	0.925	
	Fisher's exact test	-0.152	-1.369	1.063	0.791
Allo trial (% success)	Odds ratio	0.262	-0.790	1.314	
	Fisher's exact test	0.258	-0.912	1.449	0.790
Ego trial (% success)	Odds ratio	-0.331	-2.198	1.536	
	Fisher's exact test	-0.326	-2.880	1.922	1.000
Drawn path (% success)	Odds ratio	-0.916	-2.644	0.811	
	Fisher's exact test	-0.901	-3.335	1.015	0.428

Note. 'Visual' includes Place and Mixed strategies
'Extended visual' includes Place, Mixed and Other strategies

S5.b. Post-experiment interview data reported in Figure 3

A_Maze recognized

Comparison of correct response proportions

		95% Confidence Intervals		
	Log Odds Ratio	Lower	Upper	p
Odds ratio	-0.123	-1.483	1.238	
Fisher's exact test	-0.121	-1.722	1.480	1.000

B_ Landmarks (number of)

Independent Samples Mann-Whitney U test					95% CI for Rank-Biserial Correlation	
	W	p	Hodges-Lehmann Estimate	Rank-Biserial Correlation	Lower	Upper
Remembered	370.000	0.313	-1.796e-5	-0.147	-0.419	0.148
Noticed Double	369.000	0.295	-7.918e-5	-0.150	-0.421	0.146
Placed correctly	483.000	0.451	1.891e-5	0.113	-0.182	0.389

Note. For the Mann-Whitney test, effect size is given by the rank biserial correlation.

Supplementary Material S6: Distance optimization of a learned path as a measure of movement accuracy

S6.a. Distance optimization of the learned path during training

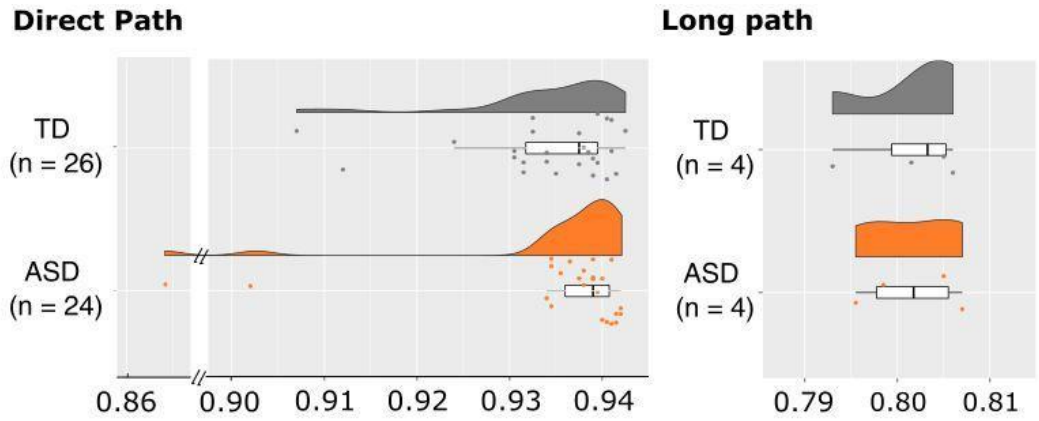

Using non parametric Mann-Whitney tests, we compared the ability to optimize the distance traveled when performing the learned path, separately for participants who learned a direct path (A4, 24 ASD: median = 0.939 [0.936-0.941] vs. 26 TD: median = 0.938 [0.932-0.940], BF_{01} = 1.84) and for those who learned a long path (A5, 4 ASD: median = 0.8030 [0.800-0.806] vs. 4 TD: median = 0.803 [0.799-0.805], BF_{01} = 1.66). Bayesian factors for both comparisons are inconclusive. Frequentist statistics (below) reveal no significant difference. ASD: autism spectrum disorder; TD: typical development.

Mann-Whitney U test				95% CI for Rank-Biserial Correlation	
	W	p	Rank-Biserial Correlation	Lower	Upper
A4	341.000	0.169	0.236	-0.093	0.518
A5	7.500	0.721	0.250	-0.584	0.827

Note. For the Mann-Whitney test, effect size is given by the rank biserial correlation.

S6.c. Distance optimization of the Ego trial

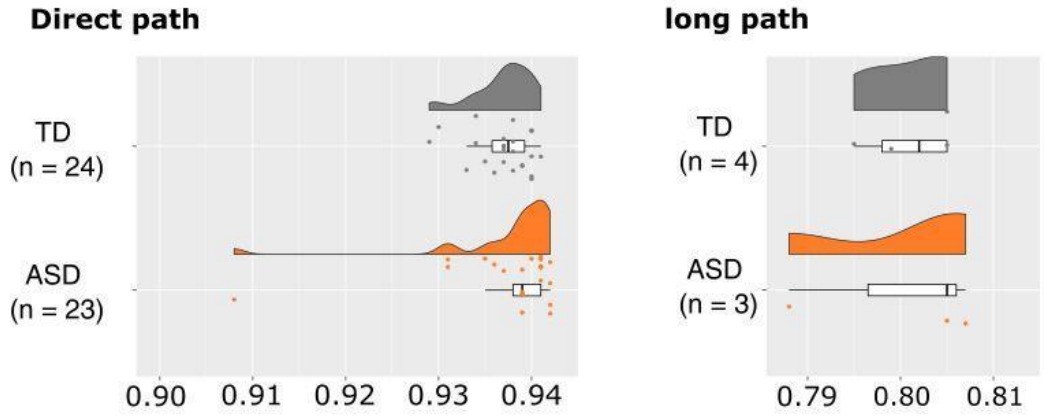

Using non parametric Mann-Whitney tests, we compared the ability to optimize the distance traveled when performing the learned path in the absence of visual landmarks (Ego trial) for participants performing a direct path (A4, 23 ASD: median = 0.939 [0.938-0.941] vs. 24 TD: median = 0.938 [0.936-0.939], BF_{01} = 0.57) and a long path (A5, 3 ASD: median = 0.805 [0.796-0.806] vs. 4 TD: median = 0.802 [0.798-0.805], BF_{01} = 1.84). The number of subjects is reduced because only those who successfully performed the Ego trial were included in this analysis. Bayesian factors for both comparisons are inconclusive. The frequentist statistics below reveal no significant difference.

Mann-Whitney U test				95% CI for Rank-Biserial Correlation	
	W	p	Rank-Biserial Correlation	Lower	Upper
A4	341.000	0.169	0.236	-0.093	0.518
A5	7.500	0.721	0.250	-0.584	0.827

Note. For the Mann-Whitney test, effect size is given by the rank biserial correlation.

Supplementary Material S7: Attention assessment test

As part of their cognitive assessment, ASD and TD participants underwent several items of the standardized Test of Attentional Performance (TAP software package, Psytest, Germany). Only parameters specified as critical are reported here. All comparisons were performed using Mann-Whitney U test. There was no difference between groups, except for the median time of correct response in verbal flexibility, which was expected in ASD (Varanda et al., 2017).

TAP scores	***ASD (n = 25)***	***TD (n = 29)***	***BF_{01}***	***Interpretation***
WM3 - omission (sd)	1.920 (2.14)	2.483 (4.13)	3.362	No difference (moderate)
VF3 - Error (sd)	*1.6 (2.47)*	2.862 (5.22)	2.085	No difference (anecdotal)
VF3 - median RT (sd)	**786ms (209)**	**622ms (149)**	**0.109**	**Difference (moderate)**
DA3 - omissions (sd)	2.0 (5.41)	1.59 (4.24)	3.268	No difference (moderate)
GO2 - errors (sd)	1.423 (3.85)*	1.034 (2.471)	2.454	No difference (anecdotal)
GO2 - median RT (sd)	532.52 (73.66)*	531.21 (56.66)	3.6	No difference (moderate)
CI - errors (sd)	1.44(3.39)	1.21(3.37)	2.884	No difference (anecdotal)
CI - omissions (sd)	0.28 (1.02)	0.24(1.12)	2.896	No difference (anecdotal)
CS - Validity effect (sd)	39.6 ms (26.2)	39.58 ms (35.65)**	3.472	No difference (moderate)
CS - Validity x position effect	18.42 ms (26.05)	17.73 ms (60.43)	1.442	Inconclusive

* ASD: n=26; ** TD n=28; median RT: Median reaction time of correct responses

WM3: Working Memory level 3; FV3: Verbal flexibility with letter/digit alternance; DA3: Divided attention II, double task; MDN TR: median reaction time of correct response; GO2: Go / No-Go task with 5 stimuli including 2 targets; CI: Intermodal comparison; CS: shifting of the attentional focus. Validity and position effects are evaluated by comparing target-related reaction times depending on cue validity and cue position (left vs. right).

Varanda, C. A., & Fernandes, F. (2017). Cognitive flexibility training intervention among children with autism: a longitudinal study. *Psicologia, reflexao e critica : revista semestral do Departamento de Psicologia da UFRGS*, *30*(1), 15. https://doi.org/10.1186/s41155-017-0069-5